Isı Bilimi ve Tekniği Dergisi, 44, 1, 163-189, 2024
J. of Thermal Science and Technology
©2024 TIBTD Printed in Turkey
ISSN 1300-3615
e-ISSN 2667-7725
https://doi.org/10.47480/isibted.1494478

THEORETICAL PERFORMANCE ASSESSMENT OF A PARABOLIC TROUGH HUMIDIFYING SOLAR COLLECTOR-BASED SOLAR STILL

Harris J.N. WELEPE *, Hüseyin GÜNERHAN **, Levent BİLİR ***
* Graduate School of Natural and Applied Sciences, Mech. Engr. Dept., Ege Uni., 35100-Bornova-Izmir,
hwelepe@gmail.com ; harrisharrismail@gmail.com, ORCID: 0000-0001-7431-9813
** Department of Mechanical Engineering, Faculty of Engineering, Ege University, 35100-Bornova-Izmir
huseyingunerhan@gmail.com, ORCID: 0000-0003-4256-2418
*** Department of Energy Systems Engineering, Faculty of Engr., Yaşar University, 35230-Bornova-Izmir
levent.bilir@yasar.edu.tr, ORCID: 0000-0002-8227-6267

(Geliş Tarihi: 04.12.2023, Kabul Tarihi: 12.05.2024)

Abstract: In this paper, a parabolic trough humidifying solar collector-based solar still (PHSC-SS) is proposed. Its purpose is to apply some important performance improvement techniques to the flat plate humidifying solar collector-based solar still (flat plate HSC-SS), to significantly improve overall system performance. These included the use of parabolic trough solar concentrators and the design of humidifying solar collectors from evacuated tube collectors. The results reveal that, unlike flat plate HSC-SS, which must operate with a turbulent airflow regime to achieve optimum overall performance, PHSC-SS must operate with a laminar airflow regime and high inlet and outlet temperatures of air (at least 55 °C and less than 100 °C, at atmospheric pressure) in the heat collector element. For 900 W/m^2 of incident solar irradiance, 2 m^2 of solar collector area, and 0,00042 kg/s of air flow rate, the maximum energy efficiency, exergy efficiency and daily freshwater productivity of PHSC-SS were found to be 68,12%, 14,87% and 1,697 kg/h, respectively. Whereas for the same incident solar irradiance and solar collector area, and 0,1 kg/s of air flow rate, those of the flat plat HSC-SS were 72,9%, 1,12%, and between 1,07 – 2,923 kg/h (for inlet and outlet temperatures of air less than 30 °C, at atmospheric pressure), respectively. Although in some extreme cases freshwater productivity of flat plate HSC-SS can be higher than that of PHSC-SS, it should be noted that laminar airflow regime confers great advantages to PHSC-SS. These are higher air temperatures at condenser inlet (which ease water condensation process), no need of an auxiliary cooling device (needed in the flat plate HSC-SS), less mechanical vibrations of system, reduced condenser size, and less energy consumed by air blowers. Furthermore, the upper limit of the PHSC-SS is a PHSC-SS that operates without air flow, but rather by vaporization of water droplets at boiling point from absorber, followed by their suction to condenser, similarly to a flash evaporation.
Keywords: seawater desalination, parabolic trough humidifying solar collector, heat collector element, energy efficiency, exergy efficiency

PARABOLİK OLUKLU NEMLENDİRİCİ GÜNEŞ KOLLEKTÖRÜ BAZLI GÜNEŞ ENERJİLİ DESALİNASYON SİSTEMİNİN TEORİK PERFORMANS DEĞERLENDİRİLMESİ

Özet: Bu makalede, parabolik oluklu nemlendirici güneş kolektörü bazlı güneş enerjili desalinasyon sistemi (PHSC-SS) önerilmektedir. Amacı, bazı önemli performans iyileştirme tekniklerini düz plaka nemlendirici güneş kolektörü bazlı desalinasyon sistemine (düz plaka HSC-SS) uygulamaktır. Genel sistem performansını önemli ölçüde iyileştirmek içindir. Bunlar arasında parabolik oluklu güneş yoğunlaştırıcılarının kullanımı ve nemlendirici güneş kolektörlerinin tahliye borulu kolektörlerden tasarlanması yer almaktadır. Sonuçlar, optimum genel performans elde etmek için türbülanslı bir hava akışı rejimiyle çalışması gereken düz plakalı HSC-SS'nin aksine, PHSC-SS'nin laminer bir hava akışı rejimiyle ve ısı kolektörü elemanında yüksek hava giriş ve çıkış sıcaklıklarıyla (atmosferik basınçta en az 55 °C ve 100 °C'den düşük) çalışması gerektiğini ortaya koymaktadır. 900 W/m^2 gelen güneş ışınımı, 2 m^2 güneş kolektörü alanı ve 0,00042 kg/s hava akış hızı için PHSC-SS'nin maksimum enerji verimi, ekserji verimi ve tatlı su üretkenliği sırasıyla %68,12, %14,87 ve 1.697 kg/saat olarak bulunmuştur. Aynı gelen güneş ışınımı, güneş kolektörü alanı, ve 0,1 kg/s hava akış hızı için düz plakalı HSC-SS'nin elde edilen değerleri sırasıyla %72,9, %1,12 ve atmosferik basınçta 30 °C'den düşük hava giriş ve çıkış sıcaklıkları için 1,07 - 2,923 kg/saat arasında olarak bulunmuştur. Bazı aşırı durumlarda düz plakalı HSC-SS'nin tatlı su verimliliği,

PHSC-SS'den daha yüksek olsa da, laminer hava akımı rejiminin PHSC-SS'ye büyük avantajlar sağladığı belirtilmelidir. Bunlar, kondenser girişindeki daha yüksek hava sıcaklıkları (suyun yoğuşma işlemi kolaylaştırması), yardımcı bir soğutma cihazına gerek olmaması (düz plakalı HSC-SS'te gereklidir), sistemin daha az mekanik titreşimi, kondenser boyutunun küçülmesi ve hava üfleyiciler tarafından daha az enerji tüketilmesidir. Ayrıca, PHSC-SS'nin üst sınırı, hava akışı olmadan çalışan bir PHSC-SS'dir. Bu sistem, kaynama noktasındaki su damlacıklarının absorberden buharlaştırılması ve ardından kondensere emilmesi ile çalışmaktadır. Bu, bir flaş buharlaşmaya benzemektedir.

Anahtar Kelimler: deniz suyu desalinasyonu, parabolik oluklu nemlendirici güneş kolektörü, ısı toplayıcı elemanı, enerji verimliliği, ekserji verimliliği

NOMENCLATURE

a : length of the collector cross-section area (m)
A : area, projection area of parabolic trough refl. (m^2)
A_k : cross-sectional area of absorber (m^2)
$A_{a,ext}$: absorber outer area (m^2)
$A_{a,int}$: absorber inner area (m^2)
$A_{e,ext}$: glass envelope outer area (m^2)
$A_{e,int}$: glass envelope inner area (m^2)
c_p : specific heat at constant pressure (J/kg.K)
c_v : specific heat at constant volume (J/kg.K)
d : diameter (m)
D_{AB} : mass diffusion coefficient of substance A into substance B (m^2/s)
D_{H_2O-air} : mass diffusion coefficient of water into air, especially liquid water from absorber surface into air passing through the collector (m^2/s)
$\dot{E}$: incident solar irradiance (W/m^2)
e_e : emissivity of glass cover or overall emissivity between the sky and the glass cover
$\dot{E}_{ex}$: incident solar exergy (W)
e_a : emissivity of absorber
e_{ae} : overall emissivity between abs. and glass envelope
f : Darcy friction factor
h_f : specific enth. of liq. water sprayed into system (J/kg)
h_{fg} : latent heat of water vaporization (J/kg)
h_g : specific enthalpy of water vapor (J/kg)
$h_{g@T_e}$: specific enth. of saturated water vapor at the glass cover temperature (J/kg)
$h_{g@T_a}$: specific enthalpy of saturated water vapor at the absorber temperature (J/kg)
h_{mass} : mass transfer coefficient (m/s)
h_{wind} : convective heat transfer coefficient resulting from wind effect ($W/m^2.K$)
h : enthalpy of moist air per unit mass of dry air ($J/kg_{(dry\ air)}$), convective heat transfer coefficient ($W/m^2.K$)
$K(i)$: incident angle modifier
k : thermal conductivity (W/m.K)
L : length of heat collector element (m)
Le: Lewis number
M : molar mass, molar mass of moist air (kg/kmol)
$\dot{m}_f$: mass flow rate of moist air (kg/s)
$\dot{m}$: dry air mass flow rate passing through the system (kg/s)
$\dot{m}_{wa,Fick'slaw}$: water evaporation rate from absorber or liquid water surface derived from Fick's law (kg/s)
$\dot{m}_{wa}$: maximum water mass flow rate that can be evaporated into the system, (kg/s)
n_b: number of brackets
Nu: Nusselt number
Nu_∞: Nusselt number for a fully developed flow
p: partial pressure (Pa), perimeter
P : total pressure (Pa), and (atm) in the expression of D_{AB}, 1 atm = 101325 Pa
p_a: partial pressure of dry air in moist air (Pa)
Pe: Peclet number
Pr: Prandlt number
$\dot{Q}$: heat transfer, total enthalpy, total enthalpy variation (W)
R_a: gas constant of dry air (J/kg.K)
Re: Reynolds number
Sc: Schmidt number
Sh: Sherwood number
s_f: entropy of liquid water sprayed into system (J/kg.K)
s_g : water vapor entropy (J/kg.K)
T : temperature (K)
y : proportion y of the water mass flow rate that reaches the abs. to the total sprayed water mass flow rate ($0 \leq y \leq 1$).

Abbreviations
ETC: evacuated tube collector
HCE: heat collector element
HDH: humidification – dehumidification
HSC-SS: humidifying solar collector-based solar still
ISD: interfacial solar desalination
MSF: multi-stage flash
PCM: phase change material
PHSC: parabolic humidifying solar collector
PHSC-SS: parabolic humidifying solar collector-based solar still
SAH/SWH-HDH: solar air and water heaters-based humidification – dehumidification
SAH: solar air heater
SAH-HDH: solar air heater-based humidification – dehumidification
SS: solar still
SWH: solar water heater
SWH-HDH: solar water heater-based humidification – dehumidification

Subscripts
0: dead state, ambient environment
1: state 1 of air, state of air at system inlet
2: state 2 of air, state of air at condenser inlet
a: absorber
abs: absorbed
amb: ambient environment
b: bracket
bb: base of bracket
ci: condenser inlet
co: condenser outlet
cond: conduction
conv: convection
e: glass envelope
evap: evaporation
ext: external
f: moist air, air flowing through the heat coll. element
g: gas in vacuum annulus (air in this study)
int: internal
opt: optical
r: reflector (parabolic trough reflector)
rad: radiation
s: sun
sat: saturated state
wa : liquid water sprayed into system

Greek symbols
α : absorptivity,
γ: product of effective optical efficiency terms
δ: molecular diameter (m)
Γ: specific heat ratio
ΔT : difference between air temperature at heat collector element outlet and inlet (K or °C)
ε : roughness of the inner wall of the collector (m)
η_{ex} : exergy efficiency
η : energy efficiency, optical efficiency
λ: mean free path (m)
μ : dynamic viscosity of moist air (kg/m.s)
ν : kinematic viscosity of moist air (m^2/s)
ρ : density, density of moist air (kg/m^3)
ρ_r: clean mirror reflectivity
σ : Stefan-Boltzmann constant ($W/m^2.K^4$)
τ_e : transmissivity of glass envelope
$\varphi(i)$: collector geometrical end losses
ψ : exergy of moist air per unit mass of dry air ($J/kg_{(dry\ air)}$)
ψ_{wa} : exergy of liquid water per unit mass (J/kg)
ω : humidity ratio of moist air ($kg_{(water)}$ / $kg_{(dry\ air)}$)
$\tilde{\omega}$: molar ratio between water vapor concentration and dry air concentration in moist air ($Mol_{(water)}$ / $Mol_{(dry\ air)}$)

INTRODUCTION

Direct solar desalination systems are among the major research on seawater desalination technologies for freshwater production. Although they are not yet used on an industrial scale because of their low productivity, they are of great interest for small-scale and low-cost freshwater production. They are characterized by the fact that seawater directly receives incident solar irradiance, heats up, and evaporates into air, unlike indirect desalination systems where it receives solar energy through heat exchangers.

Direct solar desalination systems can be classified into three technologies: solar stills (SS) (Abbaspour et al., 2022; Alatawi et al., 2022; Angappan et al., 2022; Elgendi et al., 2022; Kabeel et al., 2017; Kaushal & Varun, 2010; Muthu Manokar et al., 2014; Sampathkumar et al., 2010; Sharshir, Yang, et al., 2016), humidification–dehumidification (HDH) systems (Alnaimat et al., 2021; Chauhan et al., 2021; Kasaeian et al., 2019; M & Yadav, 2017; Rahimi-Ahar, Hatamipour, & Ahar, 2020; Santosh et al., 2019, 2022), and interfacial solar desalination systems (ISD) (Liang et al., 2021; Luo et al., 2021; Trinh et al., 2022; Wang et al., 2022). This paper is part of research for designing a solar still with improved overall performance. Solar stills have been widely developed and studied, and still attract interest because of the low cost of materials and easiness of system construction. The techniques that have been applied in earlier works to improve their performance can be summarized as follows (Welepe et al., 2022):

- modification of the shape of solar still (Durkaieswaran & Murugavel, 2015; Ghandourah et al., 2022; Kumar Chauhan & Kumar Shukla, 2022b; Mohammadi et al., 2020; Prasanna & Deshmukh, 2022; Sambare et al., 2022; Saravanakumar et al., 2022; Shanazari & Kalbasi, 2018; Siddula et al., 2022),
- heat transfer optimization by using evacuated tube collectors (ETC) (M. A. Essa et al., 2021; Shafii et al., 2016), corrugated absorber (H. Ahmed et al., 2022; Elshamy & El-Said, 2018), absorber coating (Chandrashekara & Yadav, 2017; Kumar Chauhan & Kumar Shukla, 2022a), fins on absorber (Dhivagar et al., 2022; Kabeel & Abdelgaied, 2017; Velmurugan et al., 2008; Yousef et al., 2019), porous absorber (A. F. Mohamed et al., 2019; Shah et al., 2022; Thakur et al., 2022; Yousef et al., 2019), nanofluids (Bait & Si–Ameur, 2018; Elango et al., 2015; Kabeel et al., 2014b, 2014a; Mahian et al., 2017; Meng et al., 2022; Nijmeh et al., 2005; Sharshir, Elkadeem, et al., 2020; Sharshir et al., 2017, 2019),
- the use of solar concentrators and auxiliary heat sources (Bahrami et al., 2019; Chandrashekara & Yadav, 2017; Elminshawy et al., 2015; Hashemi et al., 2020; Jafari Mosleh et al., 2015; Maliani et al., 2020; Nassar et al., 2007; Nayagam et al., 2022; Wu et al., 2017),
- water vapor mass transfer optimization from the evaporation surface to the condenser (Peng et al., 2022), and separation of condenser from evaporator to avoid water vapor condensation on glass cover, which decreases its transmissivity and therefore freshwater productivity (Al-Otoom & Al-Khalaileh, 2020; Elminshawy et al., 2015; Ibrahim & Dincer, 2015; Shoeibi, Kargarsharifabad, Rahbar, et al., 2022; Wu et al., 2017),
- preheating seawater and regulating its flow rate by using wicks (Abdelaziz et al., 2021; Abdullah et al., 2019; Abdullah, Omara, Essa, Alarjani, et al., 2021; Abdullah, Omara, Essa, Younes, et al., 2021; Dhindsa, 2021; F. A. Essa, Alawee, et al., 2021; F. A. Essa, Omara, et al., 2021; Fayaz et al., 2022; Jobrane et al., 2021, 2022; Modi, Maurya, et al., 2022; Modi, Patel, et al., 2022; Modi & Modi, 2019; Negi et al., 2022; Omara et al., 2013; Sharshir, El-Samadony, et al., 2016; Sharshir, Eltawil, et al., 2020; Younes, Abdullah, Essa, & Omara, 2021; Younes, Abdullah, Essa, Omara, et al., 2021; Zaheen Khan, 2022), water pumps (Abozoor et al., 2022; M. M. Z. Ahmed et al., 2022; Kumar et al., 2014), rotating belts (Al-Otoom & Al-Khalaileh, 2020; Saeed et al., 2022),
- glass cover cooling (Elashmawy, 2019; Kousik Suraparaju & Kumar Natarajan, 2022; Sharshir, El-Samadony, et al., 2016; Sharshir et al., 2017; Sharshir, Rozza, Joseph, et al., 2022; Sibagariang et al., 2022), s
- the use of heat storage materials such as latent heat storage or phase change material (PCM) and sensible heat storage (H. Ahmed et al., 2022; Al-harahsheh et al., 2018; Al-Harahsheh et al., 2022; Arunkumar & Kabeel, 2017; Chandrashekara & Yadav, 2017; Deshmukh & Thombre, 2017; Elashmawy & Ahmed, 2021; Jafari Mosleh & Ahmadi, 2019; Mohanraj et al., 2021; Poonia et al., 2022; Saeed et al., 2022; Shoeibi, Kargarsharifabad, Mirjalily, et al., 2022),
- breaking water surface tension by using cracked trays, air bubbles, water vaporizers, and foggers (Abed et al., 2021; Dumka & Mishra, 2020; El-Said et al., 2021; El-Said & Abdelaziz, 2020; F. A. Essa, Abdullah, et al., 2021; Fallahzadeh et al., 2020).

Many comprehensive reviews of these enhancement techniques have been conducted over time (Abbaspour et al., 2022; Alatawi et al., 2022; Angappan et al., 2022; Elgendi et al., 2022; Hussein et al., 2024; Kabeel et al., 2017; Kaushal & Varun, 2010; Mehta et al., 2024; Muthu Manokar et al., 2014; Omara, Ahmed, et al., 2024; Omara, Alawee, et al., 2024; Sampathkumar et al., 2010; Sharshir, Yang, et al., 2016). In general, most systems integrate two or more enhancement techniques (Welepe et al., 2022).

Abbaspour et al. (Abbaspour et al., 2024) investigated the efficacity of a vertical solar still (VSS), focusing on variables such as wick selection, condensate plate

wettability, and device dimensions. The research highlighted 5.1% performance enhancement with cotton wicks compared to gauze, and 34% increase in freshwater production with super hydrophilic plates over super hydrophobic ones. In addition, optimal VSS dimensions of 32 cm × 30 cm were identified. The authors declared that these findings underscore the potential for enhancing VSS efficiency, offering valuable insights for addressing global water scarcity and facilitating clean water access, with the maximum daily freshwater production rate reaching 1.250 kg per m² of solar receiver.

Mahala and Sharma (Mahala & Sharma, 2024) studied the combined impact of rectangular fins, gravels (G), and phase change material (PCM) on the efficiency of pyramid solar stills, comparing conventional solar stills (CSS) with modified ones (MSS). Experimental results, conducted in Uttar Pradesh, India, during May 2023, revealed significant improvements in daily productivity, energy, exergy efficiency, and economic and environmental parameters for MSS + G, CSS + G, and MSS, compared to CSS. Notably, MSS + G demonstrates 4.82 L/m^2 (84% increase) of daily freshwater productivity, 30.58% (81.1% increase) of maximum energy efficiency, 3.4% (273% increase) of maximum exergy efficiency, and a 0,02 $/L (29.2% reduction) of cost per liter of fresh water produced, alongside mitigating 19.14 tons of CO_2 emissions.
Saha et al. (Saha et al., 2024) experimentally studied a novel solar-energy-driven water purification system, by incorporating vacuum pressure and paraffin wax (PCM) as an energy storage material into a conventional double-slope solar still. The system was designed to enhance freshwater production in remote areas lacking grid electricity and underground water access. Experimental results demonstrated an increase of 63% in daily freshwater productivity i.e., from 5.46 L/m^2 to 7.03 L/m^2, along with 82% (28.72% enhancement) of maximum energy efficiency and 8.3% (22.43% enhancement) of maximum exergy efficiency for the modified system compared to the conventional one. These findings highlighted the potential of vacuum-pressure and PCM integration to enhance solar still performance, offering a cost-effective solution for freshwater production in resource-constrained areas.

Ziapour et al. (Ziapour et al., 2024) conducted a study on an innovative single-slope solar still desalination system with an enhanced modeling approach, aiming to address global desalination challenges. Through energy, exergy, and economic analyses, the system's performance is evaluated in cities such as Boushehr, Lisboa, Riyadh, and Tripoli. By utilizing flat reflectors and semi-transparent modules, the system achieved notable daily freshwater production values ranging from 11.15 kg/day to 15.58 kg/day across the cities. The analysis also revealed that despite promising outcomes, the system's reliance on weather conditions poses a limitation, suggesting the need for future research to minimize this dependency and scale up production capacities.

Lauvandy et al. (Lauvandy et al., 2024) designed and studied a low-cost floating solar still prototype to address water scarcity issues in rural areas, particularly on Sumba Island, Indonesia. Constructed from accessible materials like PVC pipes, mica sheets, foam blocks, and towels, the solar still is easily replicable by local communities. Testing conducted in Bandung, Sumba, and Jatiluhur Dam during the dry season demonstrated the prototype's ability to produce significant amounts of fresh water, ranging from 0.590 kg/day to 1.165 kg/day. The authors concluded that despite its effectiveness, limitations such as reduced evaporation rates due to cover saturation and warmer temperatures hindering condensation are noted, and further optimization are needed for long-term reliability and durability.

Elashmawy et al. (Elashmawy et al., 2024) investigated a tubular solar still with two troughs to enhance evaporation and energy efficiency while reducing freshwater production costs. Conducted in Suez, Egypt, the two-trough device demonstrated a significant increase in freshwater productivity (36.1%) and energy efficiency (43.46%) compared to the single-trough device. Daily freshwater productivity for the two-trough and single-trough devices were 6.83 L/m^2/day and 5.02 L/m^2/day, respectively, with energy efficiencies of 54.5% and 37.99%, respectively. Moreover, the two-trough configuration reduced water production costs by 22.3%, reaching $11.78/ton. Future research suggestions of this work include testing triple-trough configurations, investigating shadow effects, conducting deeper thermal analysis, and exploring solar concentrating techniques to further enhance tubular solar still performance.

Pandey and Naresh (Pandey & Naresh, 2024) performed experimental investigation on a modified pyramid solar still (MPSS) integrated with a pulsating heat pipe (PHP), aiming to enhance freshwater productivity, energy efficiency, and cost-effectiveness compared to conventional pyramid solar stills (CPSS). Experimental investigations conducted in Surat City, India, revealed that the MPSS consistently outperforms the CPSS. For instance, at a water depth of 2 cm, the MPSS achieved a daily freshwater productivity of approximately 4.10 L/m^2/day compared to CPSS's productivity of 3.05 L/m^2/day, with 25.51% increase in energy efficiency compared to CPSS as well. Future research directions suggested by the authors include exploring advanced heat transfer mechanisms, integrating additional enhancements like fins and phase change materials, and employing computational fluid dynamics modeling for further optimization and validation.

Amin et al. (Amin et al., 2024) integrated metallic thermal transfer constituents and parabolic trough

collectors (PTC) into passive tubular solar still configurations, alongside beeswax phase change material (PCM), to produce fresh water. The developed model combines a heat exchanger (HE) and beeswax PCM. The empirical analysis revealed a significant enhancement, with 8.06 L/m^2/day (66.18% increase) of freshwater productivity and a maximum energy efficiency of 76% (54 % average). Whereas the TSS without HE and PCM achieved a freshwater productivity and energy efficiency of 2.5 L/m^2/day and 16.10%, respectively. Finally, the authors declared these outcomes underscored the effectiveness of the developed tubular solar distillation system in consistent and reliable freshwater generation, driven by strategic integration and operational synergy.

Luo et al. (Luo et al., 2024) investigated a desalination system based on a unidirectional heat transfer solar still, integrating efficient evaporation with waste heat recovery for high energy utilization. The design optimizes light transmission and condensation functions while integrating high-performance interfacial evaporation materials and minimizing heat loss through unidirectional heat transfer. Using a self-made hydrogel sponge, outdoor experiments demonstrated an evaporation rate of 6.0 kg/m^2/h and a freshwater productivity of 4.5 kg/m^2/h under an average sunlight intensity of 1.07 kW/m^2, with potential for further improvement. The authors stated that this study contributes valuable insights into optimizing interfacial evaporative solar stills, advancing solar desalination through system structure design and evaporation material development.

Somwanshi and Shrivastava (Somwanshi & Shrivastava, 2023) studied a closed loop inclined wick solar still (CLIWSS) with an additional heat storage reservoir to address freshwater scarcity in remote regions. The CLIWSS operates in a closed loop, continuously feeding warm water back into the still. A thermal model of the CLIWSS was developed and validated, showing enhanced freshwater productivity compared to a typical Inclined Wick Solar Still (IWSS). For Jodhpur, India, the CLIWSS achieved a maximum hourly freshwater productivity of 1.025 L/m^2/h in May and 0.556 L/m^2/h in December. The total daily freshwater productivity for summer and winter was 8.432 L/m^2 and 3.618 L/m^2, respectively, representing increases of 115% and 98% compared to conventional IWSS. The CLIWSS offered a competitive and cost-effective solution for solar desalination in India, particularly for remote and small communities, according to the authors. They also conducted a similar study on a closed loop inclined wick solar still augmented with an external bottom reflector (CLIWSSR) (Somwanshi & Shrivastav, 2024). The daily freshwater productivity of the CLIWSSR in a typical winter day in Raipur, Chhattisgarh, India was 6.106 kg/m^2, whereas the that of the CLIWSS in the same day was 5.047 kg/m^2, that is, an increase of 21%.

Ahmed et al. (H. Ahmed et al., 2022) designed and studied a solar still modified with a corrugated absorber plate and PCM. As a result, the freshwater productivity of the solar still with PCM was 4.5 L/day against 4.1 L/day for the solar still without PCM.

Sharshir et al. (Sharshir, Rozza, Joseph, et al., 2022) carried out experiments on a new trapezoidal pyramid solar still augmented with multi-thermal enhancers such as hang wicks, glass cover cooling, solar concentrators, and nanofluid (copper oxide, CuO). The results showed freshwater productivity, energy and exergy efficiencies of the system compared to those of the conventional solar still were improved by 147.3%, 144.2%, and 275.5%, respectively. They also conducted a similar study (Sharshir, Rozza, Elsharkawy, et al., 2022), with TiO_2-based nanofluid. Freshwater productivities obtained were 7 L/m^2/day and 3.08 L/m^2/day for the modified pyramid and traditional solar still, respectively, with daily energy efficiencies of 83.8% and 37.87%.

Tuly et al. (Tuly et al., 2022) investigated an active double slope solar still incorporating an internal sidewall reflector, hollow circular fins, and nanoparticle (Al_2O_3) mixed PCM. The maximum freshwater productivity and maximum energy efficiency achieved were 1.853 L/day and 21.56%, respectively. Moreover, they noticed significant improvements in freshwater productivity of 61.36% and 92%, respectively, in the modified solar still with pure PCM and that modified with nanofluid mixed PCM, compared to that of the conventional solar still.

Alqsair et al. (Alqsair et al., 2022) conducted a theoretical and experimental study on a drum solar still augmented with a parabolic solar concentrator, PCM, and nanoparticles coating. As a result, they obtained a system energy efficiency of 72%, and the maximum improvement in freshwater productivity noticed was 320% compared to that of the conventional solar still.

Despite these enhancement techniques, solar stills have the disadvantage of having excess water in evaporation chamber, i.e., the amount of water that receives solar energy at each instant is much higher than the evaporation rate. In fact, this increases the time needed to reach optimal evaporation temperatures and prevents optimal energy extraction from the solar absorber, leading to an increase in energy losses to the external environment and in exergy destroyed (Welepe et al., 2022).

To resolve this issue, Welepe et al. (Welepe et al., 2022) designed a new type of solar collector, named humidifying solar collector, in which the amount of water that receives solar energy at each instant equals the evaporation rate. Then, they studied the performance of a flat plate humidifying solar collector-based solar still. As a result, freshwater productivity, energy efficiency, and exergy efficiency reached 2.9 kg/h, 73%, and 1.6%, respectively, under

900 W/m^2 of incident solar irradiance. As a conclusion of their study, they stated important recommendations to improve overall system performance. These were the use of solar concentrators (parabolic trough, parabolic dish, Fresnel mirrors) to increase the solar irradiance received by the water to evaporate, and the design of humidifying solar collectors from ETC to decrease heat losses to the ambient environment.

This paper applies these recommendations or performance enhancement techniques by designing for the first time a parabolic trough humidifying solar collector-based solar still (PHSC-SS), with an ETC as heat collector element (HCE). Like in (Welepe et al., 2022), the performance parameters that will be investigated are energy and exergy efficiencies, dry air mass flow rate required, and the maximum water flow rate that can evaporate and saturate that air. The system operates in a closed air cycle to recover the energy contained in exhausted air from condenser. In this condition, freshwater productivity equals evaporated water flow rate.

Therefore, a theoretical investigation of the PHSC-SS performance is carried out in the following. Its thermodynamic model is developed and validated, its performance is analyzed, then a comparison between its freshwater productivity and those of some solar stills previously designed and studied in the literature is presented.

METHODOLOGY AND SYSTEM DESCRIPTION

The PHSC-SS has fundamentally the same operating principle as the flat plate HSC-SS. The difference is that the PHSC-SS uses a parabolic trough solar reflector and ETC as absorber for improved performance.

Hence, thin seawater droplets are sprayed uniformly on the absorber, then heat up, evaporate, and saturate the air passing through the HCE (Welepe et al., 2022). The resulting moist air is directed to the condenser to produce fresh water. Because the system operates in a closed air/open water loop as illustrated in Figure 1, and the sprayed water amount corresponds to the maximal value that can evaporate and saturate the incoming air flow rate, freshwater productivity equals the evaporated water flow rate, which in turn equals the sprayed water flow rate since there is no liquid water discharge from HCE.

Note that this control can be achieved by an external electronic circuit and sensors, which control the values of water and air flow rates circulating in the system, and then command water pumps and air blowers. These values are dynamically provided by the resolution of thermodynamic equations in section 3.

Energy and exergy equations will be solved in the Engineering Equations Solver (EES) software. Some thermodynamic and physical properties relations, therefore, will be skipped since they are included in the source code of this software.

Figure 1 presents the schematic diagram of the PHSC-SS, which includes its main components (PHSC, Condenser) and the circulation paths of air and water. The numbers 1 and 2 on this figure represent the state of air in the psychrometric chart (See Figure 5).

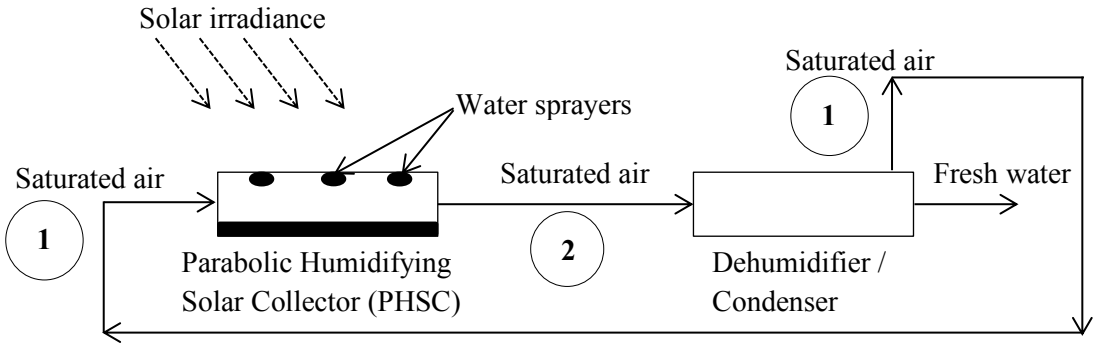

Figure 1. Schematic diagram of the PHSC-SS operating in closed air/open water loop. Adapted from (Welepe et al., 2022).

Figure 2 presents the longitudinal section view of the PHSC's HCE, with the heat and mass transfer mechanisms occurring inside and around it. This helps in establishing energy balance equations of Section 3.

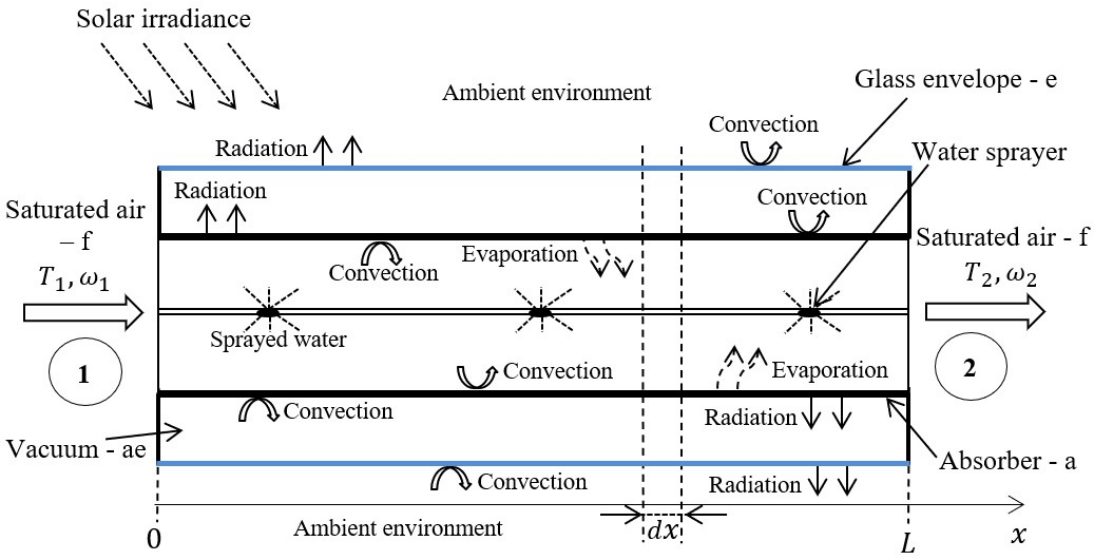

Figure 2. Longitudinal section view of the HCE of the PHSC**:** Heat and mass transfer mechanisms occurring inside and around it. Adapted from (Forristall, 2003; Padilla et al., 2011; Welepe et al., 2022; Yılmaz & Mwesigye, 2018).

Figure 3, like Figure 2, shows the heat and mass transfer mechanisms occurring inside and around the PHSC's HCE, but in a cross-sectional view, to enhance the representation of the system. Figure 4 depicts the thermal circuit of the PHSC's HCE. It is particularly useful in system thermodynamic analysis, as unlike Figures 2 and 3, it simplifies the representation of heat and mass transfer mechanisms, and therefore energy balance equations.

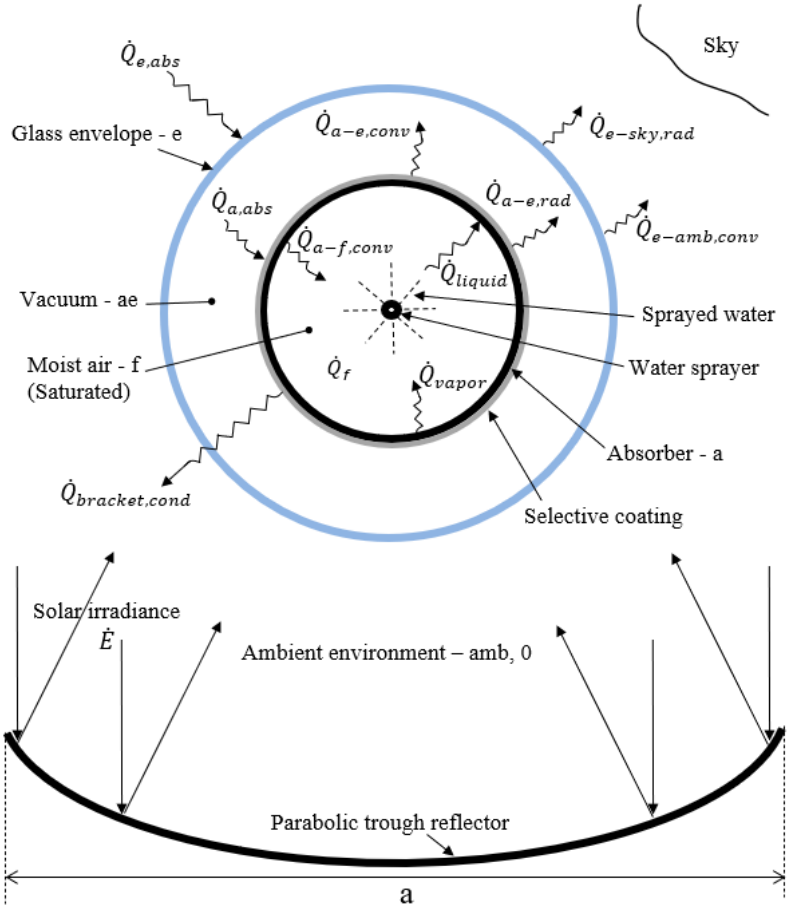

Figure 3. Cross-sectional view of the PHSC**:** Heat and mass transfer mechanisms occurring inside and around it. Adapted from (Forristall, 2003; Padilla et al., 2011; Yılmaz & Mwesigye, 2018).

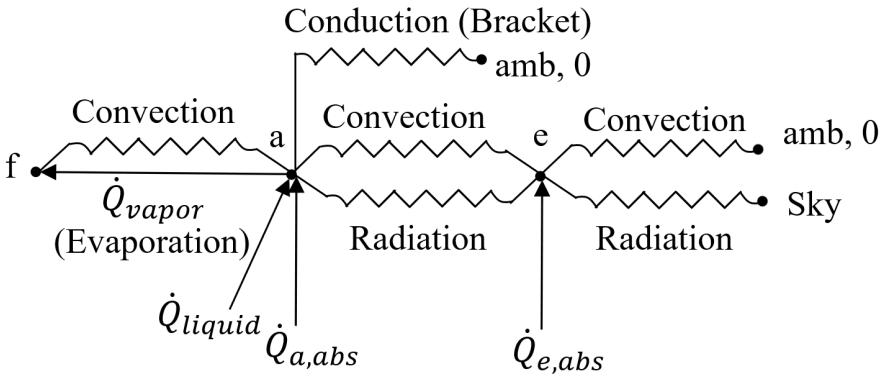

Figure 4. Thermal circuit of the PHSC. Adapted from (Forristall, 2003; Padilla et al., 2011).

As for Figure 5, it shows the psychrometric path followed by air in the PHSC-SS, operating in closed air/open water loop. In this operating scenario, air remains saturated and follows the path 1-2-1, state 1 being the desired initial state of air at the HCE inlet, and state 2 being the desired state of air at the HCE outlet.

Path 1-2: heating and humidification of air in the HCE.

Path 2-1: cooling and dehumidification of air in the condenser (direct contact condenser), with freshwater production by water vapor condensation.

To investigate the performance parameters of this system, its thermodynamic analysis must be carried out.

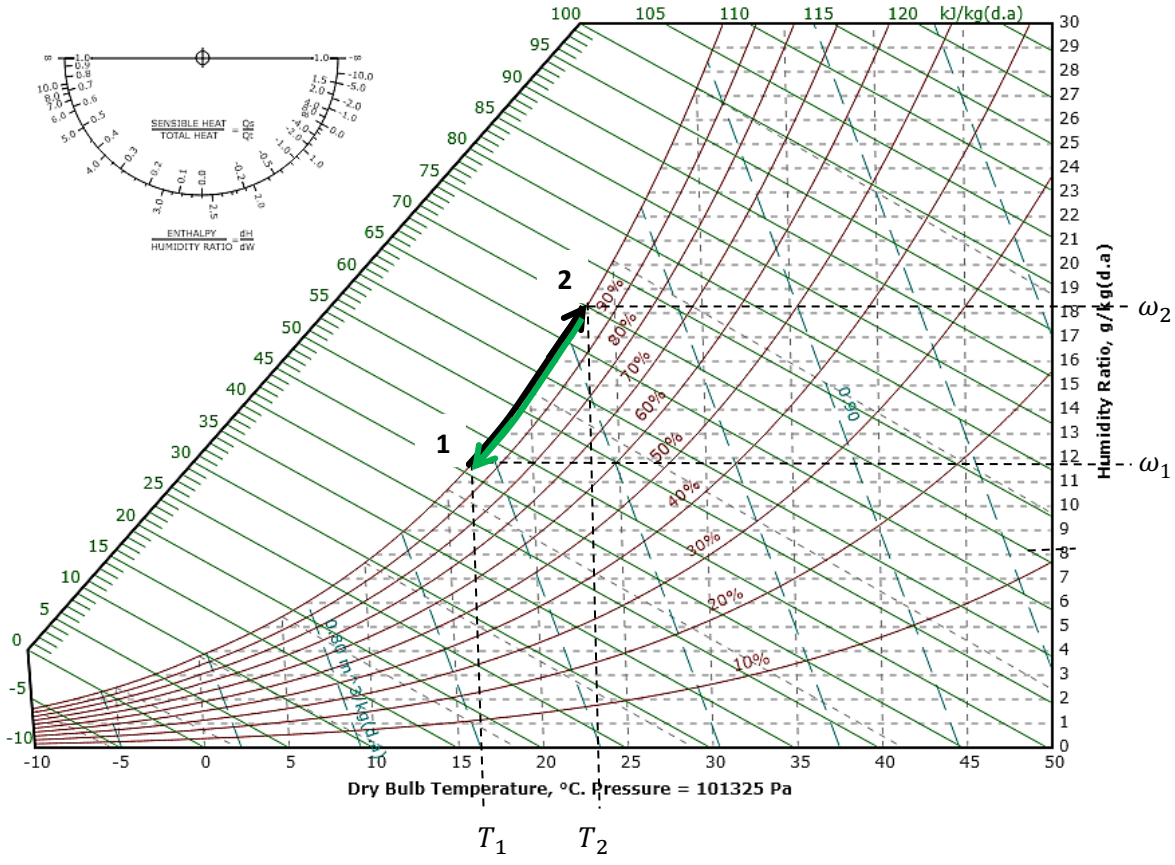

Figure 5. Air path in the PHSC-SS operating in closed air/open water loop on the psychrometric chart. Adapted from (FlyCarpet, 2021; Welepe et al., 2022).

THERMODYNAMIC ANALYSIS

Assumptions

The following assumptions are considered:

- According to Forristall (Forristall, 2003), for short parabolic solar collectors (less than 100 m in length) a 1D energy balance gives reasonable results.
- The pressure in the system is equal to atmospheric pressure. Since the system operates in a closed loop, and therefore, the internal pressure is controllable, especially under laminar air flow conditions.
- Thin water droplets sprayed into the HCE adhere to absorber surface, heat up to absorber temperature (since water depth in the HCE is negligible), and evaporate into the flowing air.
- No water droplet is carried away by the air stream, meaning that the proportion of the water mass flow rate that reaches the absorber to the total sprayed water mass flow rate equals 1.

Energy analysis of the PHSC-SS

Energy balance equations

- Energy balance equation of glass envelope

$$\dot{Q}_{e,abs} + \dot{Q}_{a-e,rad} + \dot{Q}_{a-e,conv} = \dot{Q}_{e-sky,rad} + \dot{Q}_{e-amb,conv} \quad (1)$$

- Energy balance equation of absorber

$$\dot{Q}_{a,abs} = \dot{Q}_{a-e,rad} + \dot{Q}_{a-e,conv} + \dot{Q}_{a-f,conv} + \dot{Q}_{a-f,evap} + \dot{Q}_{bracket,cond} \quad (2)$$

$$\dot{Q}_{a-f,evap} = \dot{Q}_{vapor} - \dot{Q}_{liquid} \quad (3)$$

- Energy balance equation of air flow in the PHSC

$$\dot{Q}_f = \dot{Q}_{a-f,conv} + \dot{Q}_{vapor} \quad (4)$$

Expressions of heat transfer mechanisms

Solar energy absorption

This heat transfer mechanism is expressed as follows(Padilla et al., 2011):

$$\dot{Q}_{e,abs} = \rho_r \gamma \alpha_e K(i) \varphi(i) A\dot{E}, \text{ with } A = aL \quad (5)$$

$$\dot{Q}_{a,abs} = \eta_{opt} K(i) \varphi(i) A\dot{E}, \text{ with } \eta_{opt} = \rho_r \gamma (\tau_e \alpha_a)_n \quad (6)$$

Duffie and Beckman (Duffie & Beckman, 2013) recommend the value $(\tau_e \alpha_a)_n = 1.01 \tau_e \alpha_a$.

In this study, $K(i) = 1$ and $\varphi(i) = 1$ as assumed in (Padilla et al., 2011). The factor γ is the product of effective optical efficiency terms as given below (Padilla et al., 2011):

$$\gamma = \prod_{i=1}^{6} \gamma_i \quad (7)$$

Indeed, these factors are optical imperfection factors. Their values are presented in Table 1.

Table 1. Effective optical efficiency terms (Forristall, 2003; Padilla et al., 2011).

Factor and optical properties		Symbol	Value
HCE shadowing	Luz black chrome	γ_1	0.974
	Luz cermet	γ_1	0.971
Twisting and tracking error		γ_2	0.994
Geometry accuracy of the collector mirrors		γ_3	0.980
Mirror clearness		γ_4	0.950
Dirt on HCE		γ_5	0.980
Miscellaneous factor		γ_6	0.960
Clean mirror reflectivity		ρ_r	0.935

Radiation

The below expressions are used (Yunus A. Çengel, 2011):

$$\dot{Q}_{a-e,rad} = e_{ae} A_{a,ext} \sigma (T_a^4 - T_e^4), \text{ with } e_{ae} = \left(\frac{1}{e_a} + \left(\frac{1-e_e}{e_e} \right) \left(\frac{d_{a,ext}}{d_{e,int}} \right) \right)^{-1} \quad (8)$$

$$\dot{Q}_{e-sky,rad} = e_{es} A_{e,ext} \sigma \left(T_e^4 - T_{sky}^4 \right), \text{ with } e_{es} = e_e \quad (9)$$

$$T_{sky} = 0.0552 \times T_0^{1.5} \text{ for a cloudless sky (Evangelisti et al., 2019).} \quad (10)$$

Many relations of sky temperature exist. But in general, it doesn't have a great effect in solar collector performance, unlike in radiative cooling as a passive cooling method where it has a significant effect (Duffie & Beckman, 2013). The radiative properties of different HCEs are given in Table 2.

Table 2. Radiative properties for different HCEs (Forristall, 2003).

Selective coating	Envelope transmittance	Coating absorptance	Coating emittance	
			@ 100 °C	@ 400 °C
Luz black chrome	0.935	0.94	0.11	0.27
Luz cermet	0.935	0.92	0.06	0.15
Solel UVAC cermet a	0.965	0.96	0.07	0.13
Solel UVAC cermet b	0.965	0.95	0.08	0.15
Solel UVAC cermet avg (average values)	0.965	0.955	0.075	0.14

In this work, the Solel UVAC cermet avg is considered as the HCE of the PHSC-SS, with coating emittance at 100 °C.

Convection

Convection in annulus

The annulus is filled with air under vacuum. The use of an evacuated annulus aims to minimize convective and conductive heat losses. Therefore, vacuum pressure must correspond to the free molecule regime or near free molecule conditions, i.e., approximately 0.0001 Torr (0.013 Pa) (Forristall, 2003; Padilla et al., 2011). In this case, convective heat transfer in the annulus is expressed as follows (Forristall, 2003; Padilla et al., 2011; Yılmaz & Mwesigye, 2018):

$$\dot{Q}_{a-e,conv} = h_{ae} A_{a,ext} (T_a - T_e) \quad (11)$$

$$h_{ae} = k_g/(A+B), \quad A = 0.5 d_{a,ext} \ln\left(d_{e,int}/d_{a,ext}\right), \quad B = b\lambda\left(\left(d_{e,int}/d_{a,ext}\right)+1\right) \quad (12)$$

$$b = \left(\frac{2-\alpha}{\alpha}\right)\left(\frac{9\Gamma-5}{2(\Gamma+1)}\right), \quad \Gamma = c_p/c_v \quad (13)$$

$$\lambda = \frac{1.38\times10^{-23}\times T_{ae}}{\pi\sqrt{2}\delta^2 P} \qquad T_{ae} = (T_a + T_e)/2 \quad (14)$$

The coefficient α ranges from 0.01 to nearly 1. For most gas–solid interactions the value $\alpha = 1$ could be assumed in the absence of relevant information; and for air, $\delta = 3.66 \times 10^{-10}$ m (Padilla et al., 2011).

Convection between the envelope and the ambient environment (Forristall, 2003; Padilla et al., 2011)

$$\dot{Q}_{e-amb,conv} = h_{wind} A_{e,ext} (T_e - T_{amb}) \quad (15)$$

The expression of h_{wind} depends on 'wind' and 'no wind' conditions (Forristall, 2003; Padilla et al., 2011). In this study the value 10 W/m^2.K is considered as an average value for free convection (Forristall, 2003; Padilla et al., 2011).

Convection between absorber and air (Yunus A. Çengel, 2011)

$$\dot{Q}_{a-f,conv} = h_{af} A_{a,int} \left(T_a - T_f\right), \text{ with } A_{a,int} = \pi d_{a,int} L \quad (16)$$

$$h_{af} = kNu/d_{a,int} \quad (17)$$

Nusselt, Reynolds, and Prandtl numbers are needed in evaluating h_{af}.

$$Re = \dot{m}_f d_{a,int}/A_k \mu, \quad \dot{m}_f = \dot{m}(1+\omega), \quad A_k = \pi d_{a,int}^2/4 \quad (18)$$ (Yunus A. Çengel, 2011)

The expressions of Nusselt number for short pipes are given as follows (Kakaç et al., 2012):

$$Nu = [3.66^3 + 1.61^3 (PeD_h/L)]^{1/3}, \quad Pe = RePr, \text{ for laminar air flows } (Re < 2300) \quad (19)$$

$$Nu = Nu_\infty \left[1 + (D_h/L)^{2/3}\right], \text{ for turbulent air flows} \quad (20)$$

The expression of Nu_∞ is (Kakaç et al., 2012; Yunus A. Çengel, 2011):

$$Nu_\infty = \frac{(f/8)(Re-1000)Pr}{1+12.7(f/8)^{0.5}(Pr^{2/3}-1)} \quad (21)$$

With $3 \times 10^3 < Re < 5 \times 10^6$ and $0.5 \leq Pr \leq 2000$ (Yunus A. Çengel, 2011). This relation can also be considered valid for $2300 < Re < 10^4$ (Kakaç et al., 2012).

The value of f can be evaluated from (Yunus A. Çengel, 2011):

$$\frac{1}{\sqrt{f}} \cong -1.8 \log\left[\frac{6.9}{Re} + \left(\frac{\varepsilon/D_h}{3.7}\right)^{1.11}\right] \quad (22)$$

Conduction

To be maintained at the focal point of parabolic reflectors, HCE is supported by support brackets. This contact leads to conductive heat loss to the ambient environment. To express it, each support bracket is considered as an infinite fin, whose perimeter is 0.2032 m, cross-sectional area is 1.613×10^{-4} m^2, with a thermal conductivity of 48.0 W/m.K (plain carbon steel at 600 K) as described in (Forristall, 2003; Padilla et al., 2011). In this case the expression of $\dot{Q}_{bracket,cond}$ is given as (Forristall, 2003; Yunus A. Çengel, 2011):

$$\dot{Q}_{bracket,cond} = n_b \sqrt{h_b p_b k_b A_b} (T_{bb} - T_{amb}) \text{ with } T_{bb} = T_a - 10 \text{ (Forristall, 2003), } h_b = h_{wind} \quad (23)$$

To determine the number of support brackets, it should be considered that there is a support bracket at each end of every HCE, i.e., about every 4 m of HCE's length (Forristall, 2003).

Evaporation and enthalpy variation of moist air

These heat transfer mechanisms are expressed as follows (Yunus A. Çengel, 2011):

$$\dot{Q}_f = \dot{m}(h_2 - h_1) \quad (24)$$

$$\dot{Q}_{a-f,evap} = \dot{m}_{wa}\left(h_{g@T_a} - h_{f@T_{wa}}\right), \text{ with } \dot{m}_{wa} = \dot{m}(\omega_2 - \omega_1) \quad (25)$$

$$\dot{Q}_{vapor} = \dot{m}_{wa} h_{g@T_a} \quad (26)$$

$$\dot{Q}_{liquid} = \dot{m}_{wa} h_{f@T_{wa}} \quad (27)$$

System energy efficiency

The expression of the energy efficiency of the HCE is:

$$\eta = \frac{\dot{m}h_2 - (\dot{m}h_1 + \dot{m}_{wa}h_{f@T_{wa}})}{A\dot{E}} = \frac{\dot{m}[h_2 - h_1 - (\omega_2 - \omega_1)h_{f@T_{wa}}]}{A\dot{E}},\ A = a \times L \quad (28)$$

Exergy analysis of the PHSC-SS

The expression of the exergy of moist air per unit mass of dry air is (Bejan, 2016):

$$\psi_i = (c_{p,a} + \omega_i c_{p,v})T_0\left(\frac{T_i}{T_0} - 1 - \ln\frac{T_i}{T_0}\right) + (1 + \widetilde{\omega}_i)R_a T_0 \ln\frac{P_i}{P_0} + R_a T_0\left(\widetilde{\omega}_i \ln\frac{\widetilde{\omega}_i}{\widetilde{\omega}_0} + (1 + \widetilde{\omega}_i)\ln\frac{1 + \widetilde{\omega}_0}{1 + \widetilde{\omega}_i}\right) \quad (29)$$

$$\widetilde{\omega}_i = 1.608\omega_i,\quad \widetilde{\omega}_0 = 1.608\omega_0,\quad i \in \{1, 2\}$$

The dead state is that of the outside air and the pressure in the system is considered equal to atmospheric pressure (see paragraph 3.1. for assumptions), i.e., $P_i = P_0$.

On the other hand, the expression of exergy of liquid water per unit mass is (Bejan, 2016):

$$\psi_{wa} = h_f(T_{wa}, P_0) - h_g(T_0, p_{v0}) - T_0\left(s_f(T_{wa}, P_0) - s_g(T_0, p_{v0})\right) \quad (31)$$

The expression of the exergy rate from the sun is given as (Ge et al., 2014; Jafarkazemi & Ahmadifard, 2013; Kalogirou et al., 2016; Sadaghiyani et al., 2018):

$$\dot{E}_{ex} = A\dot{E}\left(1 - \frac{4}{3}\frac{T_0}{T_s} + \frac{1}{3}\left(\frac{T_0}{T_s}\right)^4\right) \quad (32)$$

The expression of the exergy efficiency of the HCE is (Bejan, 2016):

$$\eta_{ex,ps} = \frac{exergy\ rate\ obtained\ (output)}{sum\ of\ provided\ exergy\ rates\ (input)} = \frac{\dot{m}\psi_2}{\dot{E}_{ex} + \dot{m}_{wa}\psi_{wa} + \dot{m}\psi_1} \quad (33)$$

MODEL VALIDATION

The operating principle of the flat plate HSC, as well as its thermodynamic analysis and model were detailed and validated in (Welepe et al., 2022). The same thermodynamic analysis was applied to the analysis of the PHSC. Moreover, all the specificities related to the HCE of PHSC, which have been modeled and validated in (Forristall, 2003; Padilla et al., 2011), have been scrupulously respected and their thermodynamic model applied. Consequently, it can be stated that the thermodynamic model of the PHSC used in this work is also valid and will provide reliable results. Nevertheless, it is still useful to check whether the current model follows the well-known thermodynamic law that depicts the evaporation of water from the absorber of HCE into air. That law is named Fick's law and leads the mass transfer by diffusion. In this study, it is about water diffusion into air. (30)

Although there are some simplification formulae of Fick's law, all derive from the following expressions (American Society of Heating Refrigerating and Air-Conditioning Engineers Inc. (ASHRAE), 2021; Lienhard IV & Lienhard V, 2020; Yunus A. Çengel, 2011):

$$h_{mass} = D_{AB}Sh/D_h \quad (34)$$

Sh is derived from the relations of Nu by substituting Pr with Sc.

$$Sc = \nu_f/D_{AB} \quad (35)$$

$$D_{AB} = D_{H_2O-air} = 1.87 \times 10^{-10}\left(T_f{}^{2.072}/P\right) \quad (36)$$

$$\dot{m}_{wa,Fick's\,law} = h_{mass}(\rho_{wa,a} - \rho_{vapor,f})A_{a,int} \quad (37)$$

$\rho_{wa,w}$ and $\rho_{v,f}$ are evaluated at saturation state (Welepe et al., 2022).

Figures 6, 7, and 8 present the comparison results of freshwater productivities obtained from the current model and Fick's law, for an incident solar irradiance of 900 W/m^2, 600 W/m^2, and 300 W/m^2, respectively.

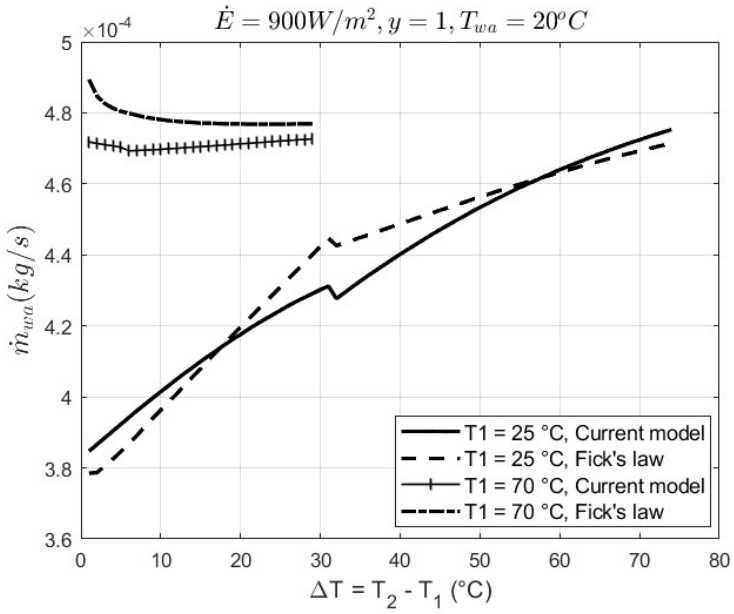

Figure 6. Comparison of freshwater productivities obtained from the current model and Fick's law, for $\dot{E} = 900\ W/m^2$.

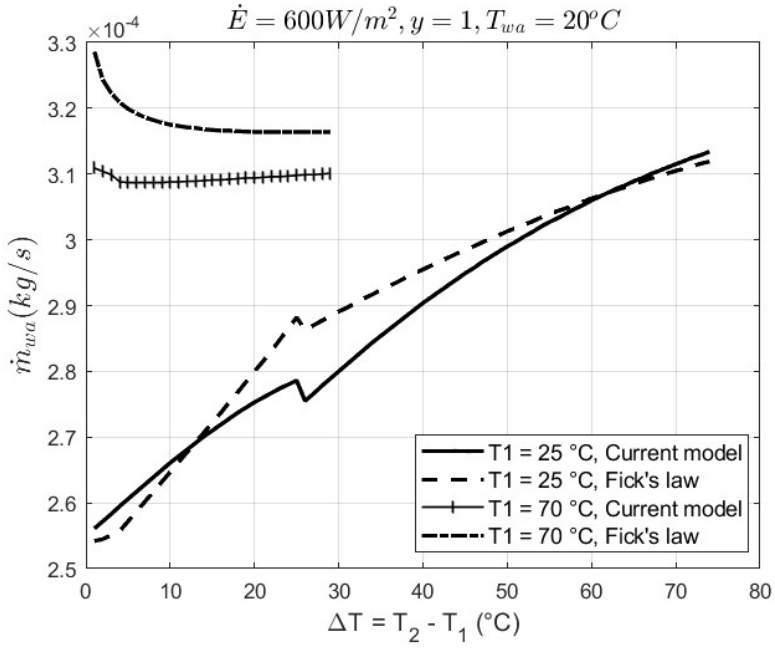

Figure 7. Comparison of freshwater productivities obtained from the current model and Fick's law, for $\dot{E} = 600\ W/m^2$.

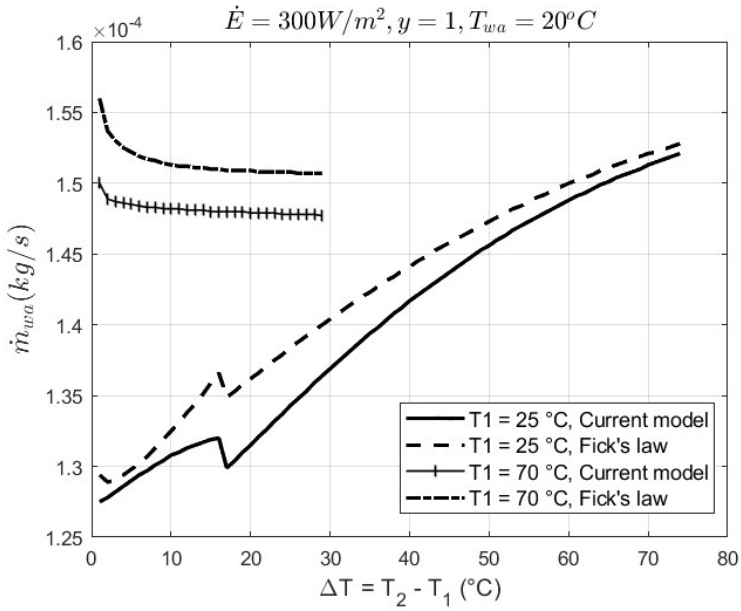

Figure 8. Comparison of freshwater productivities obtained from the current model and Fick's law, for $\dot{E} = 300\ W/m^2$.

In these figures, laminar and turbulent flow effects can be distinguished. Laminar and turbulent parts are separated by a jump or a sudden change of values (for instance, at $\Delta T \cong 31$ °C in Figure 6). Turbulent regime corresponds to the smallest ΔT values, i.e., before the jump, while laminar regime corresponds to largest ΔT values, i.e., after the jump. These figures show a good fit between the model of the HCE developed in this work and that of Fick's law. The discrepancies are acceptable for this study. This is justified by the fact that, although the study is theoretical, it is based on systems, models, and equations that have been studied and validated in earlier works [21,113,114].

RESULTS AND DISCUSSION

Performance analysis of the PHSC

Curves of performance parameters

The performance parameters investigated are energy and exergy efficiencies, the required dry air mass flow rate and the maximum water mass flow rate that can be evaporated, i.e., to be sprayed on absorber. Table 3 presents the dimensions of the PHSC, and other quantities needed to carry out the study.

The investigation is performed following three parameters which are the most important ones that can affect system performance. These are the incident solar irradiance (900 W/m^2, 600 W/m^2, 300 W/m^2), air temperature at the HCE inlet (25 °C, 40 °C, 55 °C, 70 °C), and air temperature variation between HCE inlet and outlet (1 to 74 °C, outlet temperature being less than 100 °C).

All equations were solved in EES software, and the curves of performance parameters were plotted in MATLAB software. Figures 9 – 14 present these curves.

Table 3. Dimensions of the PHSC and other quantities.

Quantity	Value (m)	Quantity	Value (m)	Quantity	Value
$d_{a,ext}$	0.097	$d_{e,int}$	0.117	n_b	2
$d_{a,int}$	0.095	a	1	T_{amb}	25 °C
$d_{e,ext}$	0.121	L	2	T_{wa}	20 °C

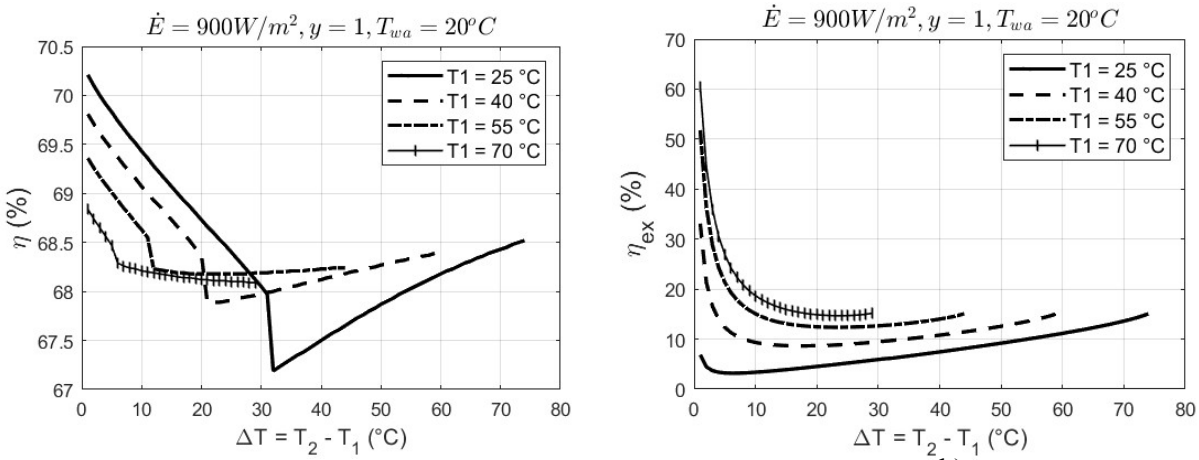

Figure 9. Performance of the PHSC for $\dot{E} = 900\ W/m^2$. a) Energy efficiency, b) Exergy efficiency.

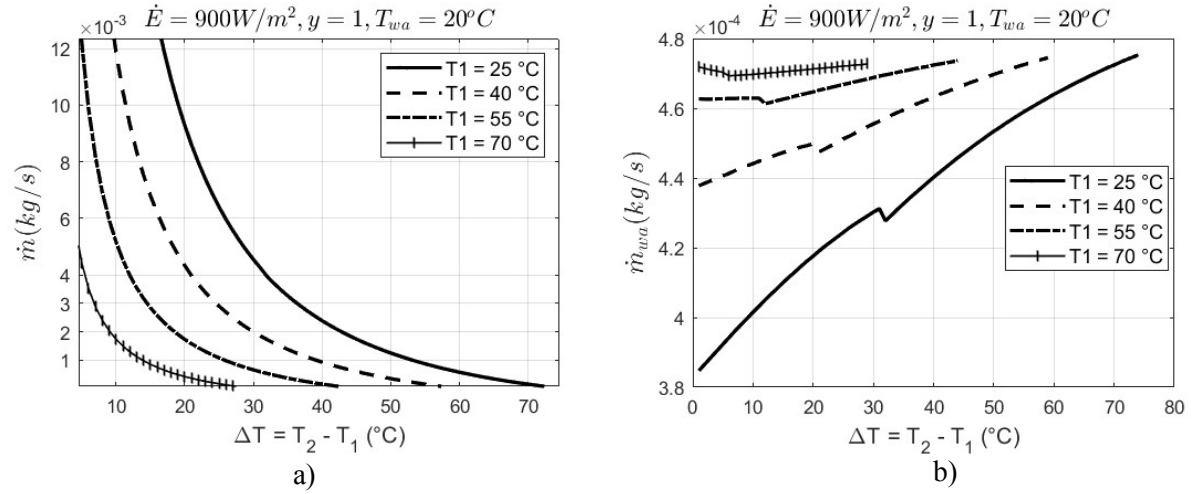

Figure 10. Performance of the PHSC for $\dot{E} = 900\ W/m^2$. a) Required air mass flow rate, b) Water mass flow rate to be sprayed.

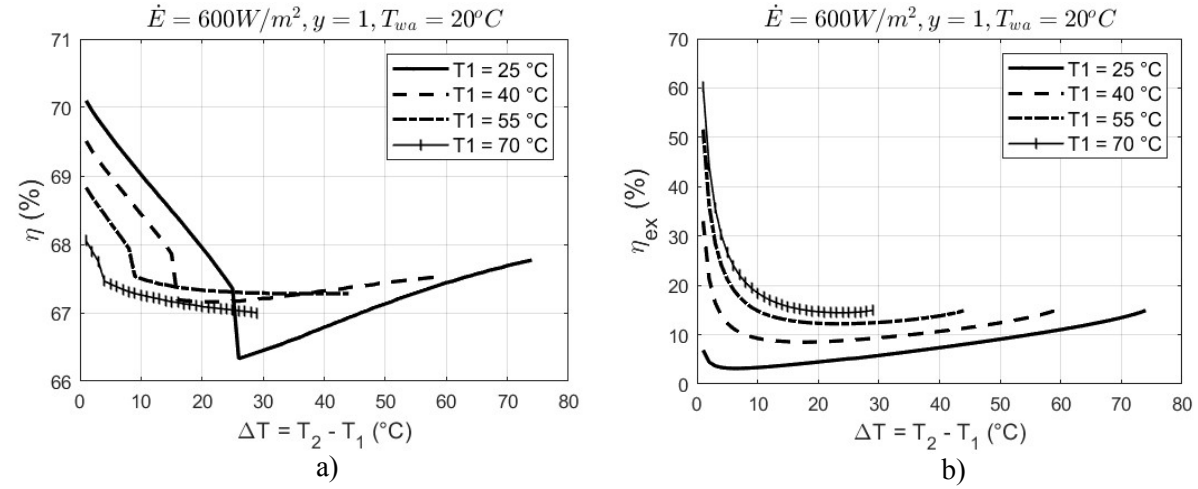

Figure 11. Performance of the PHSC for $\dot{E} = 600\ W/m^2$. a) Energy efficiency, b) Exergy efficiency.

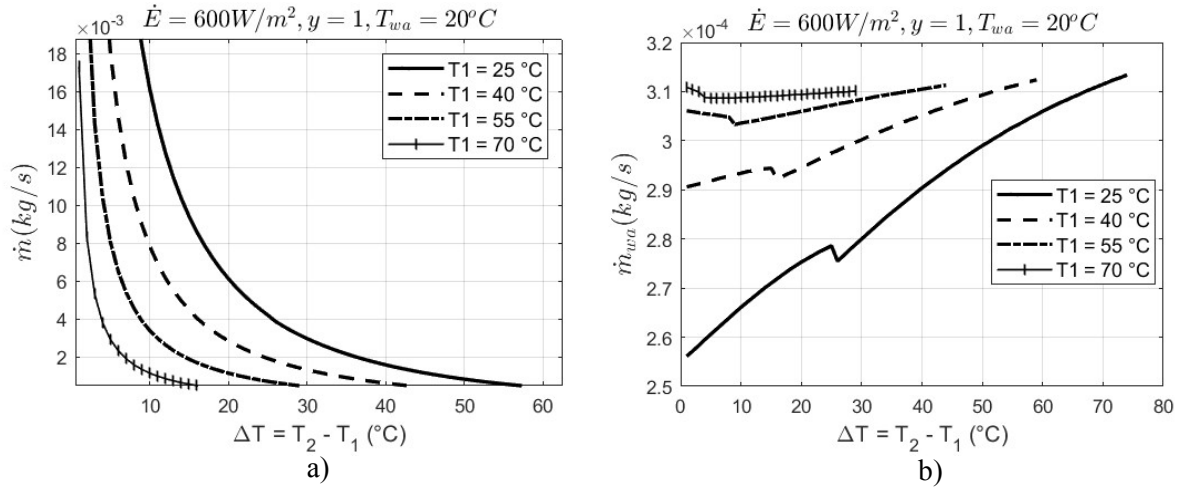

Figure 12. Performance of the PHSC for $\dot{E} = 600\ W/m^2$. a) Required air mass flow rate, b) Water mass flow rate to be sprayed.

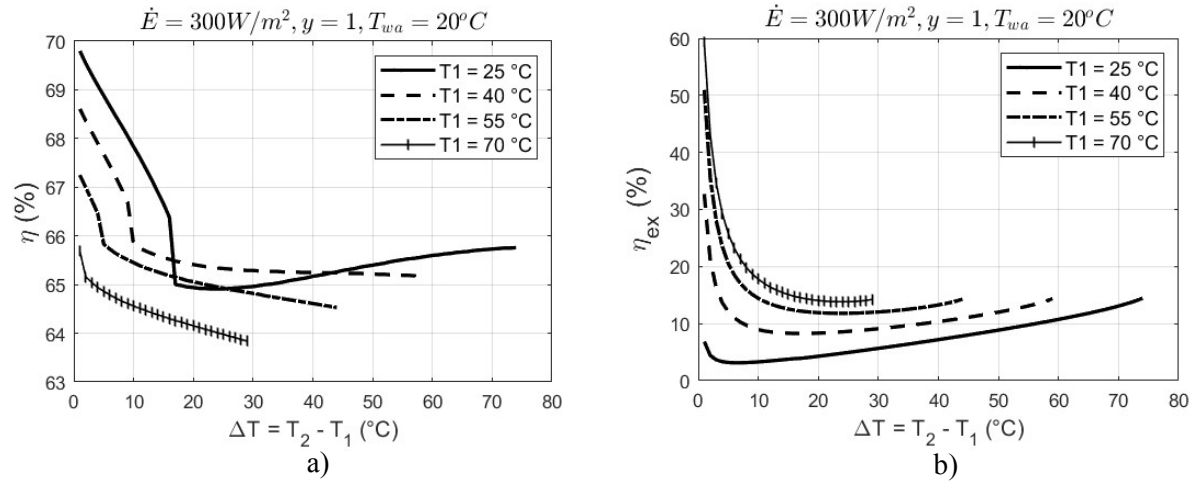

Figure 13. Performance of the PHSC for $\dot{E} = 300\ W/m^2$. a) Energy efficiency, b) Exergy efficiency.

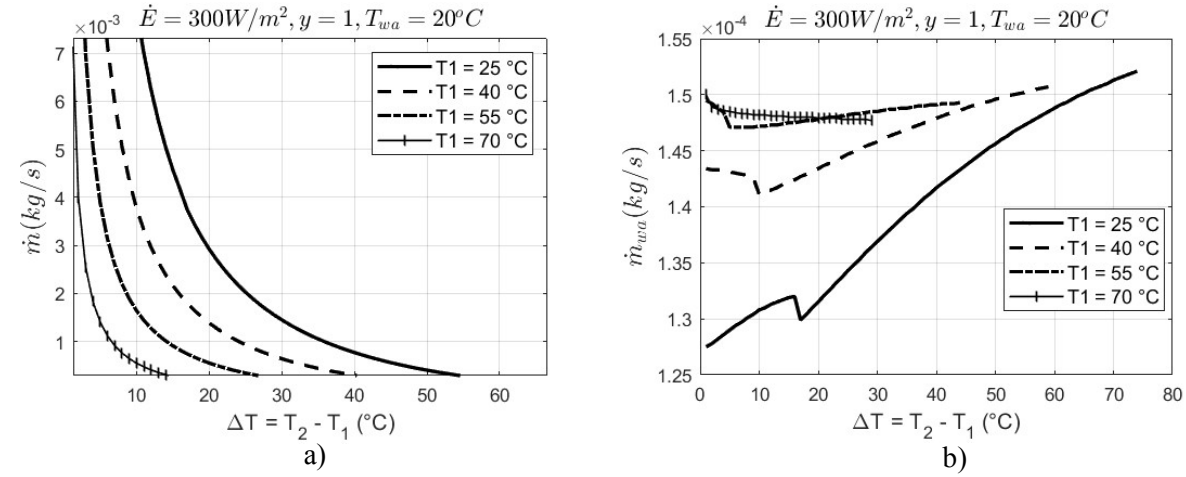

Figure 14. Performance of the PHSC for $\dot{E} = 300\ W/m^2$. a) Required air mass flow rate, b) Water mass flow rate to be sprayed.

From these curves, the effects of solar irradiance, airflow regime and air temperatures are noticeable and presented in the following sections.

Effect of solar irradiance

All performance parameters increase with solar irradiance. However, the increase in energy and exergy efficiencies is slight, i.e., a maximum difference of about 4% and 0.3% respectively, between $\dot{E} = 300\ W/m^2$ and $\dot{E} = 900\ W/m^2$.

Note that, these are efficiencies (percentages) not the values of useful energy and exergy which, on the other hand, significantly increase with solar irradiance. Whereas air and water mass flow rates almost triple from $\dot{E} = 300\ W/m^2$ to $\dot{E} = 900\ W/m^2$, i.e., almost by a proportionality ratio of solar irradiance.

This slight variation of energy and exergy efficiencies with solar irradiance is due to vacuum in the annulus of HCE, the use of low emissivity absorber and glass envelope, and water evaporation from absorber surface which minimizes absorber temperature. In fact, these efficiency enhancement techniques allow approaching the lowest levels of heat losses and exergy destroyed, i.e., system performance limit, whose percentages, therefore, remain practically constant with the variation of solar irradiance. Consequently, since air and water flow rates carry useful energy and exergy, there is a significant increase in their values with solar irradiance.

In contrast, for the flat plate HSC, all these performance parameters increase significantly with solar irradiance (Welepe et al., 2022).

Effect of airflow regime

The effects of laminar and turbulent airflow regimes can be observed on the curves of water mass flow rate to be sprayed and energy efficiency, i.e., Figures 10, 12, 14. Laminar and turbulent parts are separated by a jump or a sudden change of values. Turbulent regime corresponds to the smallest ΔT values, i.e., before the jump, while laminar regime corresponds to largest ΔT values, i.e., after the jump. The jump region corresponds to the transient regime. For example, for $T_1 = 25°\ C$, energy efficiency decreases with ΔT for turbulent airflow regime and increases for laminar airflow regime.

Furthermore, larger values of the water mass flow rate to be sprayed, which is equal to the evaporated water mass flow rate and the freshwater productivity, correspond to the smaller air mass flow rates, and therefore to a laminar air flow. This result is opposite to that of the flat plate HSC-SS studied in (Welepe et al., 2022). It is particularly important because it shows that the PHSC-SS does not need to operate with a turbulent airflow regime to produce higher amounts of fresh water, unlike the flat plate HSC-SS. A laminar regime is sufficient and necessary, allowing to process reduced air mass flow rates. Therefore, the condenser size of the PHSC-SS can be much smaller than that of the flat plate HSC-SS. In addition, smaller air mass flow rates reduce mechanical vibrations of the system and energy consumed by air blowers.

This analysis shows that the upper limit of freshwater productivity of the PHSC-SS is reached when air mass flow rate equals zero, i.e., with absorber temperature at least equal to water boiling point to cause direct evaporation of sprayed water droplets by ebullition. Thus, the upper limit of the PHSC-SS is a PHSC-SS operating without air flow, rather by ebullition and evaporation of water droplets from absorber, and suction of the resulting water vapor to condenser.

Thus, this system is similar to a flash evaporation-based desalination system like the multi-stage flash (MSF) system which is a well-known indirect solar water desalination technology. But, with the difference that in the upper limit of the PHSC-SS, water receives solar energy in the evaporation chamber (the HCE), whereas in the MSF system it receives heat in a heat exchanger before entering the evaporation chamber. This remark can justify why indirect solar desalination technologies so far offer higher freshwater productivity than that of direct solar desalination technologies.

Effect of air temperatures

For a given inlet temperature of air (T_1, temperature at HCE inlet), air and water mass flow rates decrease and increase, respectively, with its outlet temperature (T_2, temperature at HCE outlet). On the other hand, for a given outlet temperature of air, both increase with its inlet temperature. However, for high values of inlet temperature of air (from $T_1 = 55°\ C$) water mass flow rate slightly varies to become almost constant. But a small increase is still beneficial since it is the desired product. Therefore, an inlet air temperature more than 55 °C should be chosen.
This point shows that to obtain higher freshwater productivity, the system must operate with high values of inlet and outlet temperature of air. However, these temperatures must be less than the water boiling point, i.e., 100 °Cat atmospheric pressure, to remain within the validity conditions of the system operating principle and its thermodynamic model.

Combined effects of airflow regime and air temperatures

For a given inlet temperature of air (T_1), its outlet temperature (T_2, corresponding to its temperature at the condenser inlet) for a turbulent airflow regime is less than that of the laminar airflow regime. As a result, with a turbulent airflow regime, condensation of water vapor will be more difficult, since heat extraction from air in condenser strongly depends on the temperature difference between air and cooling water. For instance, with a cooling water at 20°C in condenser, the heat transfer with a

saturated air at 70°C is higher than that with a saturated air at 40°C. That is, the condensation rate of water vapor from the saturated air at 40°C is less than that from the saturated air at 70°C.

Moreover, whatever the airflow regime, system energy and exergy efficiencies range from 64.9 to 70.2% and from 3.1 to 15.1%, respectively. Unlike the flat plate HSC-SS, whose energy efficiency ranged from 28 to 73%, and whose values of more than 64.9% (minimum value for the PHSC-SS) were only obtained with highly turbulent air flows (Welepe et al., 2022).

Note that although turbulent air flows induce better energy efficiency and freshwater productivity in the flat plate HSC-SS, they involve higher air flow rates than the laminar airflow regime, leading to more mechanical vibrations of the system, more energy consumed by air blower, and larger condenser.

Additionally, they imply low air temperatures at the HSC outlet (condenser inlet), which can make difficult the water condensation process. Unlike laminar air flows in PHSC, which lead to higher air temperatures at the HCE outlet and thus condenser inlet, as shown in Figures. 9a, 11a and 13a.

Furthermore, whatever the airflow regime, exergy efficiency of the flat plate HSC ranged from 0.62 to 1.6% (Welepe et al., 2022), i.e., significantly lower than that of the PHSC (3.1 to 15.1%).

Therefore, the PHSC-SS must operate with a laminar airflow regime and high inlet and outlet temperatures of air in HCE to achieve optimum overall performance. Moreover, with a laminar airflow regime, the assumption that no water droplet is carried away by the air stream is more plausible since air flow rates are low.

COMPARISON BETWEEN THE FRESHWATER PRODUCTIVITY OF THE PHSC-SS AND THOSE OF SOME DIRECT SOLAR DESALINATION SYSTEMS IN THE LITERATURE

For a reliable result, the comparison is performed as described in (Welepe et al., 2022), i.e., for all systems, by using a proportionality ratio, freshwater productivity is estimated for the same total energy received chosen as base of calculations. This base of calculations considers incident solar energy and secondary heat sources employed for heating water and air. Omitted from the calculations is the mechanical energy generated by water pumps, air blowers, and other devices, as the pertinent values were not available in the scrutinized articles.

The base of calculations is the aggregate solar energy received per unit time by 2 m^2 of parabolic trough reflectors operating under 900 W/m^2 of solar irradiance, i.e., equivalent to1800 W (Welepe et al., 2022). The result of calculations is summarized in Table 4. In that table, the terms SAH-HDH, SWH-HDH, and SAH/SWH-HDH mean solar air heater-based HDH solar desalination system, solar water heater-based HDH solar desalination system, and solar air and water heaters-based HDH solar desalination system, respectively (Welepe et al., 2022).

Freshwater productivity of the PHSC-SS is estimated for $\dot{E} = 900\ W/m^2$, $T_1 = 70\ °C$ and $\Delta T = 20\ °C$ (i.e., $T_2 = 90\ °C$). Since it operates in a closed-air loop, and there is no liquid water discharge from HCE, amounts of water sprayed, evaporated water and condensed water (fresh water) are equal. Therefore, its freshwater productivity in kg/s can be read from Figure 10b. Its value in kg/h is given in Table 4.

Note that, in Table 4, the unit of values in column "Average freshwater productivity ($kg/m^2.h$)" is $kg/m^2.h$. However, since in some articles that have been reviewed, the total area of solar absorber plus reflectors was not provided, the unit kg/h is used and mentioned near the corresponding values.

The freshwater productivity of PHSC-SS is higher than those of most previous direct solar desalination systems.

Among systems having higher freshwater productivity than the PHSC-SS, there are:

- HSC-SS, with Tci = 27°C and Tco = 20°C. Although in this operating condition the system has higher freshwater productivity, it should be noted that it operates with turbulent air flows or higher air flow rates (0.1 kg/s in the HSC-SS against 0.00042 kg/s in the PHSC-SS for optimal performance), which imply low air temperatures at condenser inlet which make difficult the water condensation process and impose the use of an auxiliary cooling device. Since the current condenser operates with ambient water. This also leads to more mechanical vibrations of system, increase condenser size, as well as energy consumed by air blowers.

Table 4. Comparison of freshwater productivities of the PHSC-SS and some direct solar desalination systems in the literature (Welepe et al., 2022).

Authors	Type of system	Average incident solar irradiance (W/m^2)	Average total energy input (W)	Average freshwater productivity($kg/m^2.h$)	Average freshwater productivity for a total energy input of 1800 W (kg/h)	Remarks
Ghandourah et al. (Ghandourah et al., 2022)	SS	700	700	0.5 (kg/h)	1.29	Pyramid solar still with corrugated absorber plate.
Alqsair et al. (Alqsair et al., 2022)	SS	750	-	0.954	-	Use of parabolic solar concentrator, PCM, and nanoparticles coating.
Saeed et al. (Saeed et al., 2022)	SS	750	-	0.915	-	Use of corrugated drum and nano-based phase change material.
Tuly et al. (Tuly et al., 2022)	SS	400	415	0.206 (kg/h)	0.89	Active double slope solar stills incorporating internal sidewall reflector, hollow circular fins, and nanoparticle mixed PCM.
Ahmed et al. (H. Ahmed et al., 2022)	SS	480	507.36	0.19 (kg/h)	0.674	Utilization of a corrugated absorber plate and phase change material
Essa et al. (F. A. Essa, Abdullah, et al., 2021)	SS	656.75	-	0.5	1.096	Utilization of external mirrors to enhance solar energy absorption.
Essa et al. (M. A. Essa et al., 2021)	SS	682.41	-	0.48	1.270	Incorporation of an ETC with internal porous material functioning as fins, facilitating the heating of water.
Abed et al. (Abed et al., 2021)	SS	592.5	959.11	0.4	0.461	Integration of an external SWH along with four high-frequency ultrasonic vaporizers.
Al-Otoom and Al-Khalaileh (Al-Otoom & Al-Khalaileh, 2020)	SS	852.4	1278.6	4.113	8.684	Implementation of a rotating belt featuring black painted aluminum lips and a kaolin solution (hygroscopic solution) within the system.
Bahrami et al. (Bahrami et al., 2019)	SS	900	-	0.93	0.930	Deployment of a parabolic dish solar collector. Operates with boiling water.
Shafii et al. (Shafii et al., 2016)	SS	890.88		0.54	1.091	Implementation of an ETC featuring stainless-steel wool embedded within the tube for water heating.
Elminshawy et al. (Elminshawy et al., 2015)	SS	572.5	1687	2.75	2.939	Integration of 1000 W electric water heaters, complemented by external mirrors.
Abdelaziz et al. (Abdelaziz et al., 2022)	SWH/ SAH-HDH	775	3276	0.858 (kg/h)	0.471	Incorporation of an ETC as SWH, with high-frequency ultrasonic humidifier.
Alrbai et al. (Alrbai et al., 2022)	SWH-HDH	-	-	3.85 (kg/h)	-	Deployment of an ETC as a SWH, coupled with a water fogger in both the humidifier and dehumidifier.

Mohamed et al. (A. S. A. Mohamed et al., 2021)	SWH-HDH	-	5003	6.99 (kg/h)	2.515	Combination of ETC, insulated tank, auxiliary electric heater.
Rahimi-Ahar et al. (Rahimi-Ahar, Hatamipour, Ghalavand, et al., 2020)	SAH-HDH	1123	3930.5	1.8 (kg/h)	0.824	Vacuum pump to decrease humidifier pressure, and promote water evaporation. Incorporation of an ETC as a SWH, paired with a flat plate solar collector.
Zubair et al. (Zubair et al., 2017)	SWH-HDH	-	-	0.87	-	ETC is utilized as SWH.
Deniz and Çınar (Deniz & Çınar, 2016)	SAH-HDH	730.56	2483.9	-	0.439	Flat plate SAH and flat plate SWH are used.
Sharshir et al. (Sharshir, Peng, et al., 2016)	SWH-HDH	692.5	1385	1.091	2.836	ETC is utilized as SWH
	SS	692.5	775.6	0.464	1.207	Hot brine exhausted from a HDH system is used.
	SS	692.5	775.6	0.317	0.823	A conventional solar still
	Hybrid SS-HDH	692.5	2160.6	0.474	1.233	ETC is utilized as SWH in the HDH system. Solar still is fed with hot brine exhausted from HDH system.
Welepe et al. (Welepe et al., 2022) Tci = 29 °C Tco = 25 °C	HSC-SS	900	1800	0.535	1.07	A smooth duct-shaped flat plate SAH/solar collector is used. Without fins, auxiliary heat sources, or solar concentrators.
Welepe et al. (Welepe et al., 2022) Tci = 27 °C Tco = 20 °C		900	1800	1.462	2.923	
Present study	PHSC-SS	900	1800	0.848	1.697	Use of an ETC and parabolic trough reflectors, without fins and auxiliary heat sources.

- The solar still designed by Al-Otoom and Al-Khalaileh (Al-Otoom & Al-Khalaileh, 2020). In this system, heat transfer is increased by fins, and by a rotating belt which brings mechanical energy not considered in the evaluation. This system also uses a duct-shaped flat plate solar collector like in the HSC-SS and thus should require much more air flow rates than the PHSC-SS, leading to the consequences evoked in the first point.
- SWH-HDH. These systems used an ETC as SWH. That is, solar energy is only concentrated in water with fewer energy losses. Thus, the outcome can be justified by the fact that the amount of evaporated water is commensurate with the energy received by liquid water. However, larger water and air quantities are pumped, that is, larger electrical and mechanical energies are required by circulation pumps and air blowers. In addition, these systems generally use higher number of HCE (more than one), plus a separate humidification chamber (humidifier) that make them more cumbersome. Whereas, only one HCE is used in the PHSC-SS, and also serves as the system's humidifier.

The greatest advantage that PHSC-SS has in front of those systems is that it operates with laminar air flows, i.e., with lower air flow rates. This leads to higher air temperatures at condenser inlet, which eases the water condensation process, decreases mechanical vibrations of system, and lowers condenser sizes and energy consumed by air blowers.

In addition, PHSC-SS can operate with high air temperatures at HCE inlet ($T_1 = 70\ °C$ for instance). Indeed, since cooling water temperature must be lower

than air temperature at condenser outlet, i.e., HCE inlet, high air temperature at HCE inlet allows a wide range of cooling water temperatures in condenser. For instance, for $T_1 = 70\ °C$, temperature of cooling water in condenser must be less than 70 °C, while it must be less than 20 °C in HSC-SS since Tco = 20 °C, and equal to or less than the ambient temperature in most desalination systems.

Furthermore, for equal air temperatures at condenser inlet, equal cooling water temperatures in condenser, and equal air flow rates to be cooled, the water condensation process in PHSC-SS will require less cooling water quantity or flow rate than other desalination systems, and therefore less energy consumed by cooling water pump, since in PHSC-SS, air temperature at condenser outlet can be much higher than that of air at condenser outlet of other desalination systems, with optimal system performance.

Finally, since there is no water exhausted (brine) from the HCE, salt grains will crystallize on absorber surface and thus, negatively impact the performance of the PHSC-SS. Nevertheless, this can be resolved by a regular cleaning of the HCE, water-based cleaning particularly, which is part of system maintenance.

CONCLUSION

The recommendations of the study carried out by Welepe et al. (Welepe et al., 2022) on the flat plate humidifying solar collector–based solar still (flat plate HSC-SS) suggested that using solar concentrators (parabolic trough, parabolic dish, Fresnel mirrors), and designing humidifying solar collectors from evacuated tube collectors, could be very interesting deals because these techniques are known to significantly improve overall system performance. Hence, the purpose of the present study was to implement these performance improvement techniques in a parabolic trough humidifying solar collector–based solar still (PHSC-SS), and its objective was to theoretically assess system performance. The main results obtained can be stated as follows:

- Unlike flat plate HSC-SS, which must operate with a turbulent airflow regime to achieve optimum overall performance, PHSC-SS must operate with a laminar airflow regime and high inlet and outlet temperatures of air from the heat collector element (HCE) to achieve optimum overall performance. In addition, laminar airflow regime implies higher air temperatures at condenser inlet, which ease the water condensation process (thus freshwater productivity), and lowers mechanical vibrations of system, condenser size, and energy consumed by air blowers as well.
- Vacuum in annulus, low emissivity absorber and glass envelope, and especially the newly introduced enhancement technique (water evaporation from absorber surface which minimizes absorber temperature) allowed approaching system performance limit, i.e., the lowest levels of heat losses and exergy destroyed in the PHSC-SS, whose percentages, therefore, remain practically constant with the variation of solar irradiance. Consequently, since air and water flow rates carry useful energy and exergy, there is a significant increase in their values with solar irradiance.
- The upper limit of freshwater productivity of PHSC-SS is reached when air mass flow rate equals zero, i.e., with absorber temperature at least equal to water boiling point to cause direct evaporation of sprayed water droplets by ebullition. That is, the upper limit of the PHSC-SS is a PHSC-SS operating without air flow, by ebullition and evaporation of water droplets from absorber, and suction of the resulting water vapor to condenser. Thus, it is similar to a flash evaporation-based desalination system.

This last point introduces the future scope of this work. It would be interesting to design and study such a system, with attention to the effects of pressure variation on its performance, since decreasing pressure lowers water boiling point and therefore promotes water evaporation.

DECLARATION OF COMPETING INTEREST

The authors declare that they have no known competing financial interests or personal relationships that could have appeared to influence the work reported in this paper.

DECLARATION OF GENERATIVE AI AND AI-ASSISTED TECHNOLOGIES IN THE WRITING PROCESS

No AI or AI-assisted technologies were used in the writing process of this manuscript.

ACKNOWLEDGMENTS

The authors would like to thank Ege University for the software materials that helped to perform this study, as well as for the credentials giving access to a wide range of high-quality scientific journals. This research did not receive any specific grant from funding agencies in the public, commercial, or not-for-profit sectors.

REFERENCES

Abbaspour, M., Esmaili, Q., & Ramiar, A. (2024). Improving vertical solar still performance for efficient Desalination: Investigating the influence of Wick, condensate plate and device dimensions. Solar Energy, 272, 112468. https://doi.org/10.1016/j.solener.2024.112468

Abbaspour, M., Ramiar, A., & Esmaili, Q. (2022). Efficiency improvement of vertical solar stills – A review. Solar Energy, 235, 19–35. https://doi.org/10.1016/j.solener.2022.02.027

Abdelaziz, G. B., Algazzar, A. M., El-Said, E. M. S., Elsaid, A. M., Sharshir, S. W., Kabeel, A. E., & El-Behery, S. M. (2021). Performance enhancement of tubular solar still using nano-enhanced energy storage material integrated with v-

corrugated aluminum basin, wick, and nanofluid. Journal of Energy Storage, 41, 102933. https://doi.org/10.1016/j.est.2021.102933

Abdelaziz, Gamal. B., Dahab, M. A., Omara, M. A., Sharshir, S. W., Elsaid, A. M., & El-Said, E. M. S. (2022). Humidification dehumidification saline water desalination system utilizing high frequency ultrasonic humidifier and solar heated air stream. Thermal Science and Engineering Progress, 27, 101144. https://doi.org/10.1016/j.tsep.2021.101144

Abdullah, A. S., Alarjani, A., Abou Al-sood, M. M., Omara, Z. M., Kabeel, A. E., & Essa, F. A. (2019). Rotating-wick solar still with mended evaporation technics: Experimental approach. Alexandria Engineering Journal, 58(4), 1449–1459. https://doi.org/10.1016/j.aej.2019.11.018

Abdullah, A. S., Omara, Z. M., Essa, F. A., Alarjani, A., Mansir, I. B., & Amro, M. I. (2021). Enhancing the solar still performance using reflectors and sliding-wick belt. Solar Energy, 214, 268–279. https://doi.org/10.1016/j.solener.2020.11.016

Abdullah, A. S., Omara, Z. M., Essa, F. A., Younes, M. M., Shanmugan, S., Abdelgaied, M., Amro, M. I., Kabeel, A. E., & Farouk, W. M. (2021). Improving the performance of trays solar still using wick corrugated absorber, nano-enhanced phase change material and photovoltaics-powered heaters. Journal of Energy Storage, 40, 102782. https://doi.org/10.1016/j.est.2021.102782

Abed, A. H., Hoshi, H. A., & Jabal, M. H. (2021). Experimental investigation of modified solar still coupled with high-frequency ultrasonic vaporizer and phase change material capsules. Case Studies in Thermal Engineering, 28, 101531. https://doi.org/10.1016/j.csite.2021.101531

Abozoor, M. K. S., Meraj, M., Azhar, M., Khan, M. E., Seraj, M., Ahsan, M., Ahmed, S. A., & Bani Hani, E. H. (2022). Energy and exergy analyses of active solar still integrated with evacuated flat plate collector for New Delhi. Groundwater for Sustainable Development, 19, 100833. https://doi.org/10.1016/j.gsd.2022.100833

Ahmed, H., Najib, A., Zaidi, A. A., Naseer, M. N., & Kim, B. (2022). Modeling, design optimization and field testing of a solar still with corrugated absorber plate and phase change material for Karachi weather conditions. Energy Reports, 8, 11530–11546. https://doi.org/10.1016/j.egyr.2022.08.276

Ahmed, M. M. Z., Alshammari, F., Alatawi, I., Alhadri, M., & Elashmawy, M. (2022). A novel solar desalination system integrating inclined and tubular solar still with parabolic concentrator. Applied Thermal Engineering, 213, 118665. https://doi.org/10.1016/j.applthermaleng.2022.118665

Alatawi, I., Khaliq, A., Ahmed Heniegal, A. M., Abdelaziz, G. B., & Elashmawy, M. (2022). Tubular solar stills: Recent developments and future. Solar Energy Materials and Solar Cells, 242, 111785. https://doi.org/10.1016/j.solmat.2022.111785

Al-Harahsheh, M., Abu-Arabi, M., Ahmad, M., & Mousa, H. (2022). Self-powered solar desalination using solar still enhanced by external solar collector and phase change material. Applied Thermal Engineering, 206, 118118. https://doi.org/10.1016/j.applthermaleng.2022.118118

Al-harahsheh, M., Abu-Arabi, M., Mousa, H., & Alzghoul, Z. (2018). Solar desalination using solar still enhanced by external solar collector and PCM. Applied Thermal Engineering, 128, 1030–1040. https://doi.org/10.1016/j.applthermaleng.2017.09.073

Alnaimat, F., Ziauddin, M., & Mathew, B. (2021). A review of recent advances in humidification and dehumidification desalination technologies using solar energy. Desalination, 499, 114860. https://doi.org/10.1016/j.desal.2020.114860

Al-Otoom, A., & Al-Khalaileh, A. T. (2020). Water desalination using solar continuous humidification–dehumidification process using hygroscopic solutions and rotating belt. Solar Energy, 197, 38–49. https://doi.org/10.1016/j.solener.2019.12.075

Alqsair, U. F., Abdullah, A. S., & Omara, Z. M. (2022). Enhancement the productivity of drum solar still utilizing parabolic solar concentrator, phase change material and nanoparticles' coating. Journal of Energy Storage, 55, 105477. https://doi.org/10.1016/j.est.2022.105477

Alrbai, M., Hayajneh, H., Arakza, F., Enizat, J., Al-Dahidi, S., Al-Ghussain, L., & Hassan, M. A. (2022). Techno-economic analysis of a solar-powered humidification-dehumidification desalination system under fogging effect. Sustainable Energy Technologies and Assessments, 53, 102752. https://doi.org/10.1016/j.seta.2022.102752

American Society of Heating Refrigerating and Air-Conditioning Engineers Inc. (ASHRAE). (2021). 2021 ASHRAE Handbook - Fundamentals. https://www.ashrae.org

Amin, M., Umar, H., Ginting, S. F., Amir, F., Rizal, T. A., Septiadi, W. N., & Mahlia, T. M. I. (2024). Enhancing solar distillation through beeswax-infused tubular solar still with a heat exchanger using parabolic trough collector. Journal of Energy Storage, 86, 111262. https://doi.org/10.1016/j.est.2024.111262

Angappan, G., Pandiaraj, S., Panchal, H., Kathiresan, T., Ather, D., Dutta, C., Subramaniam, M. K., Muthusamy, S., Kabeel, A. E., El-Shafay, A. S., & Sadasivuni, K. K. (2022). An extensive review of performance enhancement techniques for pyramid solar still for solar thermal applications. Desalination, 532, 115692. https://doi.org/10.1016/j.desal.2022.115692

Arunkumar, T., & Kabeel, A. E. (2017). Effect of phase change material on concentric circular tubular solar still-Integration meets enhancement. Desalination, 414, 46–50. https://doi.org/10.1016/j.desal.2017.03.035

Bahrami, M., Madadi Avargani, V., & Bonyadi, M. (2019). Comprehensive experimental and theoretical study of a novel still coupled to a solar dish concentrator. Applied Thermal Engineering, 151, 77–89. https://doi.org/10.1016/j.applthermaleng.2019.01.103

Bait, O., & Si–Ameur, M. (2018). Enhanced heat and mass transfer in solar stills using nanofluids: A review. Solar Energy, 170, 694–722. https://doi.org/10.1016/j.solener.2018.06.020

Bejan, A. (2016). Advanced Engineering Thermodynamics. Wiley. https://doi.org/10.1002/9781119245964

Chandrashekara, M., & Yadav, A. (2017). An experimental study of the effect of exfoliated graphite solar coating with a sensible heat storage and Scheffler dish for desalination. Applied Thermal Engineering, 123, 111–122. https://doi.org/10.1016/j.applthermaleng.2017.05.058

Chauhan, V. K., Shukla, S. K., Tirkey, J. V., & Singh Rathore, P. K. (2021). A comprehensive review of direct solar desalination techniques and its advancements. Journal of Cleaner Production, 284, 124719. https://doi.org/10.1016/j.jclepro.2020.124719

Deniz, E., & Çınar, S. (2016). Energy, exergy, economic and environmental (4E) analysis of a solar desalination system with humidification-dehumidification. Energy Conversion and Management, 126, 12–19. https://doi.org/10.1016/j.enconman.2016.07.064

Deshmukh, H. S., & Thombre, S. B. (2017). Solar distillation with single basin solar still using sensible heat storage materials. Desalination, 410, 91–98. https://doi.org/10.1016/j.desal.2017.01.030

Dhindsa, G. S. (2021). Performance enhancement of basin solar still using paraffin wax and floating wicks in the basin. Materials Today: Proceedings, 37, 3310–3316. https://doi.org/10.1016/j.matpr.2020.09.121

Dhivagar, R., El-Sapa, S., Alrubaie, A. J., Al-khaykan, A., Chamkha, A. J., Panchal, H., El-Sebaey, M. S., & sharma, K. (2022). A case study on thermal performance analysis of a solar still basin employing ceramic magnets. Case Studies in Thermal Engineering, 39, 102402. https://doi.org/10.1016/j.csite.2022.102402

Duffie, J. A., & Beckman, W. A. (2013). Solar Engineering of Thermal Processes (4th ed.). John Wiley & Sons, Inc. https://doi.org/10.1002/9781118671603

Dumka, P., & Mishra, D. R. (2020). Performance evaluation of single slope solar still augmented with the ultrasonic fogger. Energy, 190, 116398. https://doi.org/10.1016/j.energy.2019.116398

Durkaieswaran, P., & Murugavel, K. K. (2015). Various special designs of single basin passive solar still – A review. Renewable and Sustainable Energy Reviews, 49, 1048–1060. https://doi.org/10.1016/j.rser.2015.04.111

Elango, T., Kannan, A., & Kalidasa Murugavel, K. (2015). Performance study on single basin single slope solar still with different water nanofluids. Desalination, 360, 45–51. https://doi.org/10.1016/j.desal.2015.01.004

Elashmawy, M. (2019). Effect of surface cooling and tube thickness on the performance of a high temperature standalone tubular solar still. Applied Thermal Engineering, 156, 276–286. https://doi.org/10.1016/j.applthermaleng.2019.04.068

Elashmawy, M., & Ahmed, M. M. Z. (2021). Enhancing tubular solar still productivity using composite aluminum/copper/sand sensible energy storage tubes. Solar Energy Materials and Solar Cells, 221, 110882. https://doi.org/10.1016/j.solmat.2020.110882

Elashmawy, M., Nafey, A. S., Sharshir, S. W., Abdelaziz, G. B., & Ahmed, M. M. Z. (2024). Experimental investigation of developed tubular solar still using multi-evaporator design. Journal of Cleaner Production, 443, 141040. https://doi.org/10.1016/j.jclepro.2024.141040

Elgendi, M., Kabeel, A. E., & Essa, F. A. (2022). Improving the solar still productivity using thermoelectric materials: A review. Alexandria Engineering Journal. https://doi.org/10.1016/j.aej.2022.10.011

Elminshawy, N. A. S., Siddiqui, F. R., & Addas, M. F. (2015). Experimental and analytical study on productivity augmentation of a novel solar humidification–dehumidification (HDH) system. Desalination, 365, 36–45. https://doi.org/10.1016/j.desal.2015.02.019

El-Said, E. M. S., & Abdelaziz, G. B. (2020). Experimental investigation and economic assessment of a solar still performance using high-frequency ultrasound waves atomizer. Journal of Cleaner Production, 256, 120609. https://doi.org/10.1016/j.jclepro.2020.120609

El-Said, E. M. S., Dahab, M. A., Omara, M., & Abdelaziz, G. B. (2021). Solar desalination unit coupled with a novel humidifier. Renewable Energy, 180, 297–312. https://doi.org/10.1016/j.renene.2021.08.105

Elshamy, S. M., & El-Said, E. M. S. (2018). Comparative study based on thermal, exergetic and economic analyses of a tubular solar still with semi-circular corrugated absorber. Journal of Cleaner Production, 195, 328–339. https://doi.org/10.1016/j.jclepro.2018.05.243

Essa, F. A., Abdullah, A. S., Omara, Z. M., Kabeel, A. E., & Gamiel, Y. (2021). Experimental study on the performance of trays solar still with cracks and reflectors. Applied Thermal Engineering, 188, 116652. https://doi.org/10.1016/j.applthermaleng.2021.116652

Essa, F. A., Alawee, W. H., Mohammed, S. A., Dhahad, H. A., Abdullah, A. S., & Omara, Z. M. (2021). Experimental investigation of convex tubular solar still performance using wick and nanocomposites. Case Studies in Thermal Engineering, 27, 101368. https://doi.org/10.1016/j.csite.2021.101368

Essa, F. A., Omara, Z. M., Abdullah, A. S., Kabeel, A. E., & Abdelaziz, G. B. (2021). Enhancing the solar still performance via rotating wick belt and quantum dots nanofluid. Case Studies in Thermal Engineering, 27, 101222. https://doi.org/10.1016/j.csite.2021.101222

Essa, M. A., Ibrahim, M. M., & Mostafa, N. H. (2021). Experimental parametric passive solar desalination prototype analysis. Journal of Cleaner Production, 325, 129333. https://doi.org/10.1016/j.jclepro.2021.129333

Evangelisti, L., Guattari, C., & Asdrubali, F. (2019). On the sky temperature models and their influence on buildings energy performance: A critical review. Energy and Buildings, 183, 607–625. https://doi.org/10.1016/j.enbuild.2018.11.037

Fallahzadeh, R., Aref, L., Madadi Avargani, V., & Gholamiarjenaki, N. (2020). An experimental investigation on the performance of a new portable active bubble basin solar still. Applied Thermal Engineering, 181, 115918. https://doi.org/10.1016/j.applthermaleng.2020.115918

Fayaz, Z., Dhindsa, G. S., & Sokhal, G. S. (2022). Experimental study of solar still having variable slope tilted

wick in the basin to enhance its daily yield. Materials Today: Proceedings, 48, 1421–1426. https://doi.org/10.1016/j.matpr.2021.09.195

FlyCarpet. (2021, May 7). Free Online Interactive Psychrometric Chart. http://www.flycarpet.net/en/PsyOnline

Forristall, R. (2003). Heat Transfer Analysis and Modeling of a Parabolic Trough Solar Receiver Implemented in Engineering Equation Solver. https://www.nrel.gov/docs/fy04osti/34169.pdf

Ge, Z., Wang, H., Wang, H., Zhang, S., & Guan, X. (2014). Exergy Analysis of Flat Plate Solar Collectors. Entropy, 16(5), 2549–2567. https://doi.org/10.3390/e16052549

Ghandourah, E., Panchal, H., Fallatah, O., Ahmed, H. M., Moustafa, E. B., & Elsheikh, A. H. (2022). Performance enhancement and economic analysis of pyramid solar still with corrugated absorber plate and conventional solar still: A case study. Case Studies in Thermal Engineering, 35, 101966. https://doi.org/10.1016/j.csite.2022.101966

Hashemi, S. A., Kazemi, M., Taheri, A., Passandideh-Fard, M., & Sardarabadi, M. (2020). Experimental investigation and cost analysis on a nanofluid-based desalination system integrated with an automatic dual-axis sun tracker and Fresnel lens. Applied Thermal Engineering, 180, 115788. https://doi.org/10.1016/j.applthermaleng.2020.115788

Hussein, A. K., Rashid, F. L., Rasul, M. K., Basem, A., Younis, O., Homod, R. Z., El Hadi Attia, M., Al-Obaidi, M. A., Ben Hamida, M. B., Ali, B., & Abdulameer, S. F. (2024). A review of the application of hybrid nanofluids in solar still energy systems and guidelines for future prospects. Solar Energy, 272, 112485. https://doi.org/10.1016/j.solener.2024.112485

Ibrahim, A. G. M., & Dincer, I. (2015). A solar desalination system: Exergetic performance assessment. Energy Conversion and Management, 101, 379–392. https://doi.org/10.1016/j.enconman.2015.05.060

Jafari Mosleh, H., & Ahmadi, R. (2019). Linear parabolic trough solar power plant assisted with latent thermal energy storage system: A dynamic simulation. Applied Thermal Engineering, 161, 114204. https://doi.org/10.1016/j.applthermaleng.2019.114204

Jafari Mosleh, H., Jahangiri Mamouri, S., Shafii, M. B., & Hakim Sima, A. (2015). A new desalination system using a combination of heat pipe, evacuated tube and parabolic trough collector. Energy Conversion and Management, 99, 141–150. https://doi.org/10.1016/j.enconman.2015.04.028

Jafarkazemi, F., & Ahmadifard, E. (2013). Energetic and exergetic evaluation of flat plate solar collectors. Renewable Energy, 56, 55–63. https://doi.org/10.1016/j.renene.2012.10.031

Jobrane, M., Kopmeier, A., Kahn, A., Cauchie, H.-M., Kharroubi, A., & Penny, C. (2021). Internal and external improvements of wick type solar stills in different configurations for drinking water production– A review. Groundwater for Sustainable Development, 12, 100519. https://doi.org/10.1016/j.gsd.2020.100519

Jobrane, M., Kopmeier, A., Kahn, A., Cauchie, H.-M., Kharroubi, A., & Penny, C. (2022). Theoretical and experimental investigation on a novel design of wick type solar still for sustainable freshwater production. Applied Thermal Engineering, 200, 117648. https://doi.org/10.1016/j.applthermaleng.2021.117648

Kabeel, A. E., & Abdelgaied, M. (2017). Performance enhancement of modified solar still using multi-groups of two coaxial pipes in basin. Applied Thermal Engineering, 118, 23–32. https://doi.org/10.1016/j.applthermaleng.2017.02.090

Kabeel, A. E., Arunkumar, T., Denkenberger, D. C., & Sathyamurthy, R. (2017). Performance enhancement of solar still through efficient heat exchange mechanism – A review. Applied Thermal Engineering, 114, 815–836. https://doi.org/10.1016/j.applthermaleng.2016.12.044

Kabeel, A. E., Omara, Z. M., & Essa, F. A. (2014a). Enhancement of modified solar still integrated with external condenser using nanofluids: An experimental approach. Energy Conversion and Management, 78, 493–498. https://doi.org/10.1016/j.enconman.2013.11.013

Kabeel, A. E., Omara, Z. M., & Essa, F. A. (2014b). Improving the performance of solar still by using nanofluids and providing vacuum. Energy Conversion and Management, 86, 268–274. https://doi.org/10.1016/j.enconman.2014.05.050

Kakaç, S., Liu, H., & Pramuanjaroenkij, A. (2012). Heat Exchangers: Selection, Rating, and Thermal Design (3rd ed.). CRC Press. https://doi.org/10.1201/b11784

Kalogirou, S. A., Karellas, S., Badescu, V., & Braimakis, K. (2016). Exergy analysis on solar thermal systems: A better understanding of their sustainability. Renewable Energy, 85, 1328–1333. https://doi.org/10.1016/j.renene.2015.05.037

Kasaeian, A., Babaei, S., Jahanpanah, M., Sarrafha, H., Sulaiman Alsagri, A., Ghaffarian, S., & Yan, W.-M. (2019). Solar humidification-dehumidification desalination systems: A critical review. Energy Conversion and Management, 201, 112129. https://doi.org/10.1016/j.enconman.2019.112129

Kaushal, A., & Varun. (2010). Solar stills: A review. Renewable and Sustainable Energy Reviews, 14(1), 446–453. https://doi.org/10.1016/j.rser.2009.05.011

Kousik Suraparaju, S., & Kumar Natarajan, S. (2022). Effect of Natural Sisal Fibre on Enhancing the Condensation Rate of Solar Still for Sustainable Clean Water Production. Thermal Science and Engineering Progress, 101527. https://doi.org/10.1016/j.tsep.2022.101527

Kumar Chauhan, V., & Kumar Shukla, S. (2022a). Analytical and experimental study of performance of Pyrex glass Q-dot based passive solar still glass evaporator. Thermal Science and Engineering Progress, 34, 101387. https://doi.org/10.1016/j.tsep.2022.101387

Kumar Chauhan, V., & Kumar Shukla, S. (2022b). Experimental study of effect of glass cover tilt angle of solar still in winter season of India's composite climate. Thermal Science and Engineering Progress, 33, 101348. https://doi.org/10.1016/j.tsep.2022.101348

Kumar, S., Dubey, A., & Tiwari, G. N. (2014). A solar still augmented with an evacuated tube collector in forced mode. Desalination, 347, 15–24. https://doi.org/10.1016/j.desal.2014.05.019

Lauvandy, A. F., Raihananda, F. A., Estefan, M. J., Damanik, W. S., Mu'min, G. F., Juangsa, F. B., & Sambegoro, P. (2024). Application of a low-cost floating solar still in Indonesia. Energy for Sustainable Development, 79, 101410. https://doi.org/10.1016/j.esd.2024.101410

Liang, P., Liu, S., Ding, Y., Wen, X., Wang, K., Shao, C., Hong, X., & Liu, Y. (2021). A self-floating electrospun nanofiber mat for continuously high-efficiency solar desalination. Chemosphere, 280, 130719. https://doi.org/10.1016/j.chemosphere.2021.130719

Lienhard IV, J. H., & Lienhard V, J. H. (2020). A Heat Transfer Textbook (5th ed.). Phlogiston Pres. https://ahtt.mit.edu/wp-content/uploads/2020/08/AHTTv510.pdf

Luo, X., Jiao, L., Guo, Y., Bao, H., Zhao, C., & Gu, X. (2024). Ultrahigh freshwater production achieved by unidirectional heat transfer interfacial evaporation solar still integrated with waste heat recovery. Energy Conversion and Management, 304, 118226. https://doi.org/10.1016/j.enconman.2024.118226

Luo, X., Shi, J., Zhao, C., Luo, Z., Gu, X., & Bao, H. (2021). The energy efficiency of interfacial solar desalination. Applied Energy, 302, 117581. https://doi.org/10.1016/j.apenergy.2021.117581

M, C., & Yadav, A. (2017). Water desalination system using solar heat: A review. Renewable and Sustainable Energy Reviews, 67, 1308–1330. https://doi.org/10.1016/j.rser.2016.08.058

Mahala, T., & Sharma, N. (2024). Experimental investigations of a novel solar still with heat storage materials - energy, exergy, economic and environmental analyses. Desalination, 578, 117467. https://doi.org/10.1016/j.desal.2024.117467

Mahian, O., Kianifar, A., Heris, S. Z., Wen, D., Sahin, A. Z., & Wongwises, S. (2017). Nanofluids effects on the evaporation rate in a solar still equipped with a heat exchanger. Nano Energy, 36, 134–155. https://doi.org/10.1016/j.nanoen.2017.04.025

Maliani, O. D., Bekkaoui, A., Baali, E. H., Guissi, K., El Fellah, Y., & Errais, R. (2020). Investigation on novel design of solar still coupled with two axis solar tracking system. Applied Thermal Engineering, 172, 115144. https://doi.org/10.1016/j.applthermaleng.2020.115144

Mehta, P., Bhatt, N., Bassan, G., Said, Z., & ElCheikh, A. (2024). Exploring stepped solar still developments with a case study for potable water provision in salt farming regions. Sustainable Energy Technologies and Assessments, 64, 103700. https://doi.org/10.1016/j.seta.2024.103700

Meng, Z., Li, Z., Li, Y., Zhang, C., Wang, K., Yu, W., Wu, D., Zhu, H., & Li, W. (2022). Novel nanofluid based efficient solar vaporization systems with applications in desalination and wastewater treatment. Energy, 247, 123513. https://doi.org/10.1016/j.energy.2022.123513

Modi, K. V., Maurya, S. R., Parmar, J. H., Kalsariya, A. B., & Panasara, P. B. (2022). An experimental investigation of the effectiveness of partially and fully submerged metal hollow-fins and jute cloth wick-fins on the performance of a dual-basin single-slope solar still. Cleaner Engineering and Technology, 6, 100392. https://doi.org/10.1016/j.clet.2021.100392

Modi, K. V., & Modi, J. G. (2019). Performance of single-slope double-basin solar stills with small pile of wick materials. Applied Thermal Engineering, 149, 723–730. https://doi.org/10.1016/j.applthermaleng.2018.12.071

Modi, K. V., Patel, U. N., Patel, S. J., Patel, J. N., & Patel, S. R. (2022). Efficacy of partially and fully submerged circular cross-section metal hollow-fins and black cotton cloth wick-segments on a single-basin dual-slope solar still. Journal of Cleaner Production, 344, 131059. https://doi.org/10.1016/j.jclepro.2022.131059

Mohamed, A. F., Hegazi, A. A., Sultan, G. I., & El-Said, E. M. S. (2019). Augmented heat and mass transfer effect on performance of a solar still using porous absorber: Experimental investigation and exergetic analysis. Applied Thermal Engineering, 150, 1206–1215. https://doi.org/10.1016/j.applthermaleng.2019.01.070

Mohamed, A. S. A., Shahdy, A. G., & Salem Ahmed, M. (2021). Investigation on solar humidification dehumidification water desalination system using a closed-air cycle. Applied Thermal Engineering, 188, 116621. https://doi.org/10.1016/j.applthermaleng.2021.116621

Mohammadi, K., Taghvaei, H., & Rad, E. G. (2020). Experimental investigation of a double slope active solar still: Effect of a new heat exchanger design performance. Applied Thermal Engineering, 180, 115875. https://doi.org/10.1016/j.applthermaleng.2020.115875

Mohanraj, M., Karthick, L., & Dhivagar, R. (2021). Performance and economic analysis of a heat pump water heater assisted regenerative solar still using latent heat storage. Applied Thermal Engineering, 196, 117263. https://doi.org/10.1016/j.applthermaleng.2021.117263

Muthu Manokar, A., Kalidasa Murugavel, K., & Esakkimuthu, G. (2014). Different parameters affecting the rate of evaporation and condensation on passive solar still – A review. Renewable and Sustainable Energy Reviews, 38, 309–322. https://doi.org/10.1016/j.rser.2014.05.092

Nassar, Y. F., Yousif, S. A., & Salem, A. A. (2007). The second generation of the solar desalination systems. Desalination, 209(1–3), 177–181. https://doi.org/10.1016/j.desal.2007.04.039

Nayagam, V. S., Geetha, K., Vallikannu, R., Muthuvel, S. K., Ram, G. C., Gupta, P., Sudhakar, M., Mohanavel, V., & Sathyamurthy, R. (2022). Energy efficient tubular solar still for augmented yield using electrical heater. Energy Reports, 8, 959–964. https://doi.org/10.1016/j.egyr.2022.10.283

Negi, A., Dhindsa, G. S., & Sehgal, S. S. (2022). Experimental investigation on single basin tilted wick solar still integrated with flat plate collector. Materials Today:

Proceedings, 48, 1439–1446. https://doi.org/10.1016/j.matpr.2021.09.210

Nijmeh, S., Odeh, S., & Akash, B. (2005). Experimental and theoretical study of a single-basin solar sill in Jordan. International Communications in Heat and Mass Transfer, 32(3–4), 565–572. https://doi.org/10.1016/j.icheatmasstransfer.2004.06.006

Omara, Z. M., Ahmed, M. M. Z., Alawee, W. H., Shanmugan, S., & Elashmawy, M. (2024). A comprehensive review of nano-enhanced phase change materials on solar stills with scientometric analysis. Results in Engineering, 22, 102088. https://doi.org/10.1016/j.rineng.2024.102088

Omara, Z. M., Alawee, W. H., Basem, A., & Jawad Al-Bayati, A. D. (2024). Heat loss reduction techniques for walls in solar stills: A review. Results in Engineering, 22, 101996. https://doi.org/10.1016/j.rineng.2024.101996

Omara, Z. M., Eltawil, M. A., & ElNashar, E. A. (2013). A new hybrid desalination system using wicks/solar still and evacuated solar water heater. Desalination, 325, 56–64. https://doi.org/10.1016/j.desal.2013.06.024

Padilla, R. V., Demirkaya, G., Goswami, D. Y., Stefanakos, E., & Rahman, M. M. (2011). Heat transfer analysis of parabolic trough solar receiver. Applied Energy, 88(12), 5097–5110. https://doi.org/10.1016/j.apenergy.2011.07.012

Pandey, N., & Naresh, Y. (2024). A comprehensive 4E (energy, exergy, economic, environmental) analysis of novel pyramid solar still coupled with pulsating heat pipe: An experimental study. Renewable Energy, 225, 120227. https://doi.org/10.1016/j.renene.2024.120227

Peng, G., Xu, Z., Ji, J., Sun, S., & Yang, N. (2022). A study on the upper limit efficiency of solar still by optimizing the mass transfer. Applied Thermal Engineering, 213, 118664. https://doi.org/10.1016/j.applthermaleng.2022.118664

Poonia, S., Singh, A. K., & Jain, D. (2022). Performance evaluation of PCM based solar concentrator type desalination device. Materials Today: Proceedings. https://doi.org/10.1016/j.matpr.2022.02.637

Prasanna, Y. S., & Deshmukh, S. S. (2022). Energy, exergy and economic analysis of an air cavity appended passive solar still of different basin material at varying depth. Energy for Sustainable Development, 71, 13–26. https://doi.org/10.1016/j.esd.2022.09.008

Rahimi-Ahar, Z., Hatamipour, M. S., & Ahar, L. R. (2020). Air humidification-dehumidification process for desalination: A review. Progress in Energy and Combustion Science, 80, 100850. https://doi.org/10.1016/j.pecs.2020.100850

Rahimi-Ahar, Z., Hatamipour, M. S., Ghalavand, Y., & Palizvan, A. (2020). Comprehensive study on vacuum humidification-dehumidification (VHDH) desalination. Applied Thermal Engineering, 169, 114944. https://doi.org/10.1016/j.applthermaleng.2020.114944

Sadaghiyani, O., Boubakran, M., & Hassanzadeh, A. (2018). Energy and exergy analysis of parabolic trough collectors. International Journal of Heat and Technology, 36(1), 147–158. https://doi.org/10.18280/ijht.360120

Saeed, A. A., Alharthi, A. M., Aldosari, K. M., Abdullah, A. S., Essa, F. A., Alqsair, U. F., Aljaghtham, M., & Omara, Z. M. (2022). Improving the drum solar still performance using corrugated drum and nano-based phase change material. Journal of Energy Storage, 55, 105647. https://doi.org/10.1016/j.est.2022.105647

Saha, S., Sarker, M. R. I., Kader, M. A., Ahmed, M. M., Tuly, S. S., & Mustafi, N. N. (2024). Development of a vacuum double-slope solar still for enhanced freshwater productivity. Solar Energy, 270, 112385. https://doi.org/10.1016/j.solener.2024.112385

Sambare, R. K., Dewangan, S. K., Gupta, P. K., & Joshi, S. (2022). Energy, exergy and economic analyses of Tubular solar still with various transparent cover materials. Process Safety and Environmental Protection. https://doi.org/10.1016/j.psep.2022.10.064

Sampathkumar, K., Arjunan, T. V., Pitchandi, P., & Senthilkumar, P. (2010). Active solar distillation—A detailed review. Renewable and Sustainable Energy Reviews, 14(6), 1503–1526. https://doi.org/10.1016/j.rser.2010.01.023

Santosh, R., Arunkumar, T., Velraj, R., & Kumaresan, G. (2019). Technological advancements in solar energy driven humidification-dehumidification desalination systems - A review. Journal of Cleaner Production, 207, 826–845. https://doi.org/10.1016/j.jclepro.2018.09.247

Santosh, R., Lee, H.-S., & Kim, Y.-D. (2022). A comprehensive review on humidifiers and dehumidifiers in solar and low-grade waste heat powered humidification-dehumidification desalination systems. Journal of Cleaner Production, 347, 131300. https://doi.org/10.1016/j.jclepro.2022.131300

Saravanakumar, R., Venugopal, J., Udagani, C., Thiyagarajan, V., Kumar, S. K. N., Karnan, L., Kabeel, A. E., Madhu, B., & Sathyamurthy, R. (2022). A mini review on recent advancements in inclined solar still. Energy Reports, 8, 641–645. https://doi.org/10.1016/j.egyr.2022.09.174

Shafii, M. B., Jahangiri Mamouri, S., Lotfi, M. M., & Jafari Mosleh, H. (2016). A modified solar desalination system using evacuated tube collector. Desalination, 396, 30–38. https://doi.org/10.1016/j.desal.2016.05.030

Shah, R., Makwana, M., Makwana, N., & Desai, R. (2022). Perfromance analysis of black gravel solar still. Materials Today: Proceedings. https://doi.org/10.1016/j.matpr.2022.09.115

Shanazari, E., & Kalbasi, R. (2018). Improving performance of an inverted absorber multi-effect solar still by applying exergy analysis. Applied Thermal Engineering, 143, 1–10. https://doi.org/10.1016/j.applthermaleng.2018.07.021

Sharshir, S. W., Elkadeem, M. R., & Meng, A. (2020). Performance enhancement of pyramid solar distiller using nanofluid integrated with v-corrugated absorber and wick: An experimental study. Applied Thermal Engineering, 168, 114848. https://doi.org/10.1016/j.applthermaleng.2019.114848

Sharshir, S. W., El-Samadony, M. O. A., Peng, G., Yang, N., Essa, F. A., Hamed, M. H., & Kabeel, A. E. (2016).

Performance enhancement of wick solar still using rejected water from humidification-dehumidification unit and film cooling. Applied Thermal Engineering, 108, 1268–1278. https://doi.org/10.1016/j.applthermaleng.2016.07.179

Sharshir, S. W., Eltawil, M. A., Algazzar, A. M., Sathyamurthy, R., & Kandeal, A. W. (2020). Performance enhancement of stepped double slope solar still by using nanoparticles and linen wicks: Energy, exergy and economic analysis. Applied Thermal Engineering, 174, 115278. https://doi.org/10.1016/j.applthermaleng.2020.115278

Sharshir, S. W., Kandeal, A. W., Ismail, M., Abdelaziz, G. B., Kabeel, A. E., & Yang, N. (2019). Augmentation of a pyramid solar still performance using evacuated tubes and nanofluid: Experimental approach. Applied Thermal Engineering, 160, 113997. https://doi.org/10.1016/j.applthermaleng.2019.113997

Sharshir, S. W., Peng, G., Wu, L., Yang, N., Essa, F. A., Elsheikh, A. H., Mohamed, S. I. T., & Kabeel, A. E. (2017). Enhancing the solar still performance using nanofluids and glass cover cooling: Experimental study. Applied Thermal Engineering, 113, 684–693. https://doi.org/10.1016/j.applthermaleng.2016.11.085

Sharshir, S. W., Peng, G., Yang, N., El-Samadony, M. O. A., & Kabeel, A. E. (2016). A continuous desalination system using humidification – dehumidification and a solar still with an evacuated solar water heater. Applied Thermal Engineering, 104, 734–742. https://doi.org/10.1016/j.applthermaleng.2016.05.120

Sharshir, S. W., Rozza, M. A., Elsharkawy, M., Youns, M. M., Abou-Taleb, F., & Kabeel, A. E. (2022). Performance evaluation of a modified pyramid solar still employing wick, reflectors, glass cooling and TiO2 nanomaterial. Desalination, 539, 115939. https://doi.org/10.1016/j.desal.2022.115939

Sharshir, S. W., Rozza, M. A., Joseph, A., Kandeal, A. W., Tareemi, A. A., Abou-Taleb, F., & Kabeel, A. E. (2022). A new trapezoidal pyramid solar still design with multi thermal enhancers. Applied Thermal Engineering, 213, 118699. https://doi.org/10.1016/j.applthermaleng.2022.118699

Sharshir, S. W., Yang, N., Peng, G., & Kabeel, A. E. (2016). Factors affecting solar stills productivity and improvement techniques: A detailed review. Applied Thermal Engineering, 100, 267–284. https://doi.org/10.1016/j.applthermaleng.2015.11.041

Shoeibi, S., Kargarsharifabad, H., Mirjalily, S. A. A., & Muhammad, T. (2022). Solar district heating with solar desalination using energy storage material for domestic hot water and drinking water – Environmental and economic analysis. Sustainable Energy Technologies and Assessments, 49, 101713. https://doi.org/10.1016/j.seta.2021.101713

Shoeibi, S., Kargarsharifabad, H., Rahbar, N., Khosravi, G., & Sharifpur, M. (2022). An integrated solar desalination with evacuated tube heat pipe solar collector and new wind ventilator external condenser. Sustainable Energy Technologies and Assessments, 50, 101857. https://doi.org/10.1016/j.seta.2021.101857

Sibagariang, Y. P., Napitupulu, F. H., Kawai, H., & Ambarita, H. (2022). Investigation of the effect of a solar collector, nozzle, and water cooling on solar still double slope. Case Studies in Thermal Engineering, 40, 102489. https://doi.org/10.1016/j.csite.2022.102489

Siddula, Sundeep., Stalin, N., Mahesha, C. R., Dattu, V. S. N. C. H., S, H., Singh, D. P., Mohanavel, V., & Sathyamurthy, R. (2022). Triangular and single slope solar stills: Performance and yield studies with different water mass. Energy Reports, 8, 480–488. https://doi.org/10.1016/j.egyr.2022.10.225

Somwanshi, A., & Shrivastav, R. (2024). Enhancement in the performance of closed loop inclined wick solar still by attaching external bottom reflector. Desalination and Water Treatment, 317, 100063. https://doi.org/10.1016/j.dwt.2024.100063

Somwanshi, A., & Shrivastava, R. (2023). Thermal analysis of a closed loop inclined wick solar still (CLIWSS) with an additional heat storage water reservoir. Solar Energy, 262, 111902. https://doi.org/10.1016/j.solener.2023.111902

Thakur, A. K., Sathyamurthy, R., Saidur, R., Velraj, R., Lynch, I., & Aslfattahi, N. (2022). Exploring the potential of MXene-based advanced solar-absorber in improving the performance and efficiency of a solar-desalination unit for brackish water purification. Desalination, 526, 115521. https://doi.org/10.1016/j.desal.2021.115521

Trinh, V.-H., Nguyen, N.-A., Omelianovych, O., Dao, V.-D., Yoon, I., Choi, H.-S., & Keidar, M. (2022). Sustainable desalination device capable of producing freshwater and electricity. Desalination, 535, 115820. https://doi.org/10.1016/j.desal.2022.115820

Tuly, S. S., Ayon, A. B. S., Hassan, R., Das, B. K., Khan, R. H., & Sarker, M. R. I. (2022). Performance investigation of active double slope solar stills incorporating internal sidewall reflector, hollow circular fins, and nanoparticle-mixed phase change material. Journal of Energy Storage, 55, 105660. https://doi.org/10.1016/j.est.2022.105660

U.S. Particle Accelerator School Education in Beam Physics and Accelerator Technology. (2015). Vacuum Science and Technology for Accelerator Vacuum Systems. USPAS - Vacuum Fundamentals. https://uspas.fnal.gov/materials/15ODU/Session1_Fundamentals.pdf

Velmurugan, V., Gopalakrishnan, M., Raghu, R., & Srithar, K. (2008). Single basin solar still with fin for enhancing productivity. Energy Conversion and Management, 49(10), 2602–2608. https://doi.org/10.1016/j.enconman.2008.05.010

Wang, Q., Wang, L., Song, S., Li, Y., Jia, F., Feng, T., & Hu, N. (2022). Flexible 2D@3D Janus evaporators for high-performance and continuous solar desalination. Desalination, 525, 115483. https://doi.org/10.1016/j.desal.2021.115483

Welepe, H. J. N., Günerhan, H., & Bilir, L. (2022). Humidifying solar collector for improving the performance of direct solar desalination systems: A theoretical approach. Applied Thermal Engineering, 216, 119043. https://doi.org/10.1016/j.applthermaleng.2022.119043

Wu, G., Zheng, H., Ma, X., Kutlu, C., & Su, Y. (2017). Experimental investigation of a multi-stage humidification-dehumidification desalination system heated directly by a cylindrical Fresnel lens solar concentrator. Energy

Conversion and Management, 143, 241–251. https://doi.org/10.1016/j.enconman.2017.04.011

Yılmaz, İ. H., & Mwesigye, A. (2018). Modeling, simulation and performance analysis of parabolic trough solar collectors: A comprehensive review. Applied Energy, 225, 135–174. https://doi.org/10.1016/j.apenergy.2018.05.014

Younes, M. M., Abdullah, A. S., Essa, F. A., & Omara, Z. M. (2021). Half barrel and corrugated wick solar stills – Comprehensive study. Journal of Energy Storage, 42, 103117. https://doi.org/10.1016/j.est.2021.103117

Younes, M. M., Abdullah, A. S., Essa, F. A., Omara, Z. M., & Amro, M. I. (2021). Enhancing the wick solar still performance using half barrel and corrugated absorbers. Process Safety and Environmental Protection, 150, 440–452. https://doi.org/10.1016/j.psep.2021.04.036

Yousef, M. S., Hassan, H., & Sekiguchi, H. (2019). Energy, exergy, economic and enviroeconomic (4E) analyses of solar distillation system using different absorbing materials. Applied Thermal Engineering, 150, 30–41. https://doi.org/10.1016/j.applthermaleng.2019.01.005

Yunus A. Çengel. (2011). Heat and Mass Transfer: A Practical Approach, 3rd Edition.

Zaheen Khan, M. (2022). Diffusion of single-effect vertical solar still fixed with inclined wick still: An experimental study. Fuel, 329, 125502. https://doi.org/10.1016/j.fuel.2022.125502

Ziapour, B. M., Afzal, S., Mahdian, J., & Reza Miroliaei, A. (2024). Enhancing solar still performance through innovative modeling, integration with reflectors, and semi-transparent solar cells: A 3E analysis and multi-objective optimization. Applied Thermal Engineering, 242, 122464. https://doi.org/10.1016/j.applthermaleng.2024.122464

Zubair, M. I., Al-Sulaiman, F. A., Antar, M. A., Al-Dini, S. A., & Ibrahim, N. I. (2017). Performance and cost assessment of solar driven humidification dehumidification desalination system. Energy Conversion and Management, 132, 28–39. https://doi.org/10.1016/j.enconman.2016.10.005